1   Title: Constitutive AP2γ deficiency reduces postnatal hippocampal neurogenesis and
2   induces behavioral deficits in juvenile mice that persist during adulthood

4   Running title: AP2γ on postnatal plasticity and behavior

6   **Eduardo Loureiro-Campos**[1,2]*, **Nuno Dinis Alves**[1,2,α,*], **António Mateus-Pinheiro**[1,2],
7   **Patrícia Patrício**[1,2], **Carina Soares-Cunha**[1,2], **Joana Silva**[1,2], **Vanessa Morais Sardinha**[1,2],
8   **Bárbara Mendes-Pinheiro**[1,2], **Tiago Silveira-Rosa**[1,2], **Ana João Rodrigues**[1,2], **João Filipe**
9   **Oliveira**[1,2,3], **Nuno Sousa**[1,2] and **Luísa Pinto**[1,2,#]

11   1. Life and Health Sciences Research Institute (ICVS, School of Medicine, University of Minho,
12   Braga, Portugal

14   2. ICVS/3B's -PT Government Associate Laboratory, Braga/Guimarães, Portugal

16   3. IPCA-EST-2Ai, Polytechnic Institute of Cávado and Ave, Applied Artificial Intelligence
17   Laboratory, Campus of IPCA, Barcelos, Portugal

20   α   Current affiliation: Department of Psychiatry, Columbia University, New York, NY 10032,
21   USA; New York State Psychiatric Institute, New York, NY 10032, USA
22   *   Eduardo Loureiro-Campos and Nuno Dinis Alves contributed equally to this work and are
23   joint first authors.

25   #   Correspondence to: luisapinto@med.uminho.pt;
26   Life and Health Sciences Research Institute (ICVS), School of Medicine, University of Minho,
27   Campus de Gualtar, 4710-057 Braga, Portugal; tel: +351 253604929

1

28 **Abstract:**

29   The transcription factor activating protein two gamma (AP2γ) is an important regulator of

30   neurogenesis both during embryonic development as well as in the postnatal brain, but its role for

31   neurophysiology and behavior at distinct postnatal periods is still unclear. In this work, we

32   explored the neurogenic, behavioral, and functional impact of a constitutive AP2γ heterozygous

33   deletion in mice from early postnatal development until adulthood. Constitutive AP2γ

34   heterozygous deletion in mice caused a reduction of hippocampal transient amplifying progenitors

35   (TAPs) in the postnatal brain, inducing significant impairments on hippocampal-dependent

36   emotional- and cognitive-behavioral tasks including anxiety-like behavior and cognitive deficits,

37   typically associated with an intact neurogenic activity. Moreover, AP2γ deficiency impairs dorsal

38   hippocampus-to-prefrontal cortex functional connectivity.

39   We observed a progressive and cumulative impact of constitutive AP2γ deficiency on the

40   hippocampal glutamatergic neurogenic process, as well as alterations on limbic-cortical

41   connectivity, together with impairments on emotional and cognitive behaviors from juvenile to

42   adult periods. Collectively, the results herein presented demonstrate the importance of AP2γ in

43   the generation of glutamatergic neurons in the postnatal brain and its impact on behavioral

44   performance.

45

46   **Keywords:** Hippocampal neurogenesis, AP2γ, anxiety, cognition, spectral coherence.

2

47 **Introduction**:

48   New cells are continuously generated, differentiated into neurons, and integrated into the

49 preexisting neural networks in restricted regions of the postnatal mice brain (Boldrini et al., 2018;

50 Dennis et al., 2016; Kempermann et al., 2018; Moreno-Jiménez et al., 2019; Tobin et al., 2019).

51 One of these so-called neurogenic niches is the subgranular zone (SGZ) of the hippocampal

52 dentate gyrus (DG). Here, neural stem cells (NSC) give rise to mature neural cells including

53 glutamatergic granular neurons in a fined and tuned process with many developmental steps

54 sensitive to different regulatory influences (Kempermann et al., 2004; Mateus-Pinheiro et al.,

55 2017; Tobin et al., 2019; Toda et al., 2019). Postnatal hippocampal glutamatergic neurogenesis

56 exhibits a regulatory transcriptional sequence (Sox2$\rightarrow$ Pax6$\rightarrow$ Ngn2$\rightarrow$ AP2$\gamma$$\rightarrow$ Tbr2$\rightarrow$ NeuroD$\rightarrow$

57 Tbr1) that recapitulates the hallmarks of the embryonic glutamatergic neurogenic process in the

58 cerebral cortex (Hochgerner et al., 2018; Mateus-Pinheiro et al., 2017; Nacher et al., 2005).

59 Transcriptional factors as Pax6, Ngn2, Tbr2, NeuroD, and Tbr1 have several and distinct roles in

60 proliferation, cell kinetics, fate specification, and axonal growth (Englund, 2005; Götz et al., 1998;

61 Hevner, 2019; Hevner et al., 2006; Hochgerner et al., 2018).

62   Despite several efforts to understand the complex transcriptional network orchestration

63 involved in the regulation of neurogenesis, both in early developmental stages and during

64 adulthood, these are still to be fully understood (Bertrand et al., 2002; Brill et al., 2009; Englund,

65 2005; Hack et al., 2005; Hsieh, 2012; Mateus-Pinheiro et al., 2017; Waclaw et al., 2006).

66 Recently, the transcription factor activating protein 2 gamma (AP2γ, also known as Tcfap2c or

67 Tfa2c) was described to be an important regulator of glutamatergic neurogenesis in the adult

68 hippocampus, being involved in the regulation of transient amplifying progenitors (TAPs) cells

69 (Hochgerner et al., 2018; Mateus-Pinheiro et al., 2018, 2017). AP2γ belongs to the AP2 family of

70 transcription factors that is highly involved in several systems and biological processes, such as

71 cell proliferation, adhesion, developmental morphogenesis, tumor progression and cell fate

72 determination (Eckert et al., 2005; Hilger-Eversheim et al., 2000; Thewes et al., 2010). In addition,

73 AP2γ is functionally relevant during embryonic neocortical development, playing detrimental roles

74 in early mammalian extraembryonic development and organogenesis (Pinto et al., 2009). AP2γ is

75 critical for the specification of glutamatergic neocortical neurons and their progenitors, acting as

76 a downstream target of Pax6 and being involved in the regulation of Tbr2 and NeuroD basal

77 progenitors' determinants (Mateus-Pinheiro et al., 2017; Pinto et al., 2009). Strikingly, in humans,

78 defects in the AP2γ gene were reported in patients with severe pre- and post-natal growth

79 retardation (Geneviève et al., 2005), and to be involved in the mammary, ovarian and testicular

80 carcinogenesis (Hoei-Hansen et al., 2004; Li et al., 2002; Ødegaard et al., 2006).

81   AP2γ deletion during embryonic development results in a specific reduction of upper layer

82 neurons in the occipital cerebral cortex, while its overexpression increases region- and time-

83 specific generation of neurons from cortical layers II/III (Pinto et al., 2009). AP2γ expression

84 persists in the adult hippocampus, particularly in a sub-population of TAPs acting as a positive

85 regulator of the cell fate modulators, Tbr2 and NeuroD, and therefore as a promoter of proliferation

86 and neuronal differentiation (Mateus-Pinheiro et al., 2017). Conditional and specific

87 downregulation of AP2γ in the adult brain NSCs decreases the generation of new neurons in the

88 hippocampal DG and disrupts the electrophysiological synchronization between the hippocampus

89 and the medial prefrontal cortex (mPFC). Furthermore, mice with AP2γ conditional deletion

90 exhibited behavioral impairments, particularly a deficient performance in cognitive-related tasks

91 (Mateus-Pinheiro et al., 2018, 2017).

92   These studies reveal the crucial modulatory role of AP2γ during embryonic cerebral cortex

93 development as well as its influence on glutamatergic neurogenesis and hippocampal-dependent

94 behaviors during adulthood. Still, it is important to identify the longitudinal postnatal relevance of

95 AP2γ to brain neurophysiology and behavior. Thus, in the present study, we explored the

96 neurogenic, behavioral and functional impact of constitutive AP2γ heterozygous deletion in mice

97 since early postnatal development until adulthood. We revealed a progressive impact of AP2γ

98 deficiency on the hippocampal glutamatergic neurogenic process, alterations on limbic-cortical

99 connectivity, accompanied by behavioral impairments on emotional and cognitive modalities from

100 juvenile period to adulthood.

101

4

Results:

Constitutive AP2γ deficiency decreases proliferation and neurogenesis in the postnatal DG, without affecting neuronal morphology

We sought to dissect the impact of constitutive and heterozygous deficiency of AP2γ in the modulation of postnatal neuronal plasticity in the hippocampus, including its effect in the hippocampal neurogenic niche and in the morphology of pre-existing DG granule neurons at different postnatal periods. In juvenile and adult mice, we assessed the expression of markers for different cell populations along the neurogenic process through western blot and immunofluorescence, and the morphology of granule neurons in the DG using the Golgi-Cox staining method (Figure 1A and B). We observed a significant decrease in the expression levels of AP2γ protein in the hippocampal DG of juvenile (Figure 1C) and adult (Figure 1D) AP2$\gamma^{+/-}$ mice, with concomitant reduction of Pax6 and Tbr2 protein levels, but not Sox2, an upstream regulator of AP2γ (Mateus-Pinheiro et al., 2017).

Analysis of cell populations in the hippocampal neurogenic niche using BrdU and doublecortin (DCX) labelling (Figure 1E) revealed that the number of BrdU$^+$ and BrdU$^+$DCX$^+$ cells is reduced in both juvenile and adult AP2$\gamma^{+/-}$ mice, suggesting a decrease in the number of fast proliferating cells (transient amplifying progenitor cells (TAPs) and neuroblasts, respectively (Figure 1F-I). Of note, we observed a decrease in these cell populations with age in both WT and AP2$\gamma^{+/-}$ mice in agreement with previous reports (Kase et al., 2020; Katsimpardi and Lledo, 2018) (BrdU$^+$: Supplementary Figure 1A; BrdU$^+$DCX$^+$: Supplementary Figure 1B). In contrast, and despite an increased length (Supplementary Figure 1C) and neuronal arborization (Supplementary Figure 1D) of DG granular neurons with age, constitutive deficiency of AP2γ does not impact neither the dendritic length (Figure 1J-K), nor the neuronal complexity, in both postnatal periods (Supplementary Figure 1D).

These results highlight that AP2γ modulatory actions in the hippocampal neurogenic niche are similar and maintained in juvenile and adult mice. AP2γ transcription factor regulates NSCs proliferation and neuronal differentiation in the postnatal hippocampus by interacting with the different modulators involved in the transcriptional regulation of postnatal hippocampal neurogenesis.

AP2$\gamma^{+/-}$ mice display normal early postnatal development but anxiety-like behavior and cognitive impairments at juvenile period

In light of the negative impact of AP2γ heterozygous deficiency in the postnatal neurogenic process in the hippocampus, known as an important modulator of emotional and cognitive functions (Christian et al., 2014; Toda et al., 2019), we assessed early postnatal development and the behavioral performance of WT and AP2$\gamma^{+/-}$ at juvenile and adult periods.

5

138   Evaluation of early postnatal development was performed through the assessment of

139   somatic and neurobiological paraments during the first 21 postnatal days (Supplementary Figure

140   2). Despite a variation in the eye-opening day, responsiveness in sensory-motor functions,

141   vestibular area-dependent tasks, and strength, as well somatic parameters were similar in WT

142   and AP2$\gamma^{+/-}$ mice. Furthermore, all analyzed parameters were within the previously described

143   range (Guerra-Gomes et al., 2020; Heyser, 2003). These observations suggest that constitutive

144   heterozygous deletion of AP2γ has no impact on early postnatal development.

145   In juvenile mice (between PND 25-31), we performed the open-field (OF) test to assess

146   locomotor and anxiety-like behavior, tail suspension test (TST) and sucrose splash test (SST) to

147   assess behavioral despair and anhedonic-like behavior, and the object recognition test (ORT) to

148   assess memory (Figure 2A). In the OF, juvenile AP2$\gamma^{+/-}$ mice exhibited a lower distance traveled

149   in the anxiogenic center of the arena in comparison to WT animals (Figure 2B) suggesting an

150   anxiety-like phenotype. Of note, WT and AP2$\gamma^{+/-}$ mice display similar average velocities when

151   performing the test, indicating no changes in locomotor activity (Supplementary Figure 3A).

152   Assessment of behavioral despair and anhedonic-like behavior revealed no impact of constitutive

153   AP2γ heterozygous deletion in these emotional domains, as no alterations were observed in the

154   immobility time in the TST (Figure 2C) and grooming time in the SST (Figure 2D). Notably, despite

155   no differences in the novel object location (Figure 2E and F), AP2$\gamma^{+/-}$ mice displayed significant

156   deficits in the novel object recognition, as denoted by a decreased preference to explore the novel

157   object (Figure 2G).

158   These observations suggest that despite no evident impact on early postnatal

159   development, constitutive AP2γ heterozygous deficiency leads to memory impairments and an

160   anxious-like phenotype at juvenile period.

161

162   **AP2$\gamma^{+/-}$ adult mice exhibit significant impairments in emotional and cognitive behavioral**

163   **modalities**

164   At adulthood, behavioral assessment included OF test and elevated plus-maze (EPM) to

165   evaluate anxiety-like behavior, forced swimming test (FST) and TST to examine behavioral

166   despair, and ORT, contextual fear conditioning (CFC) and Morris water maze (MWM) to evaluate

167   cognitive performance (Figure 3A). In the OF test, AP2$\gamma^{+/-}$ mice showed a trend towards a

168   decrease in the distance traveled in the anxiogenic center of the arena (p = 0.05, Figure 3B), with

169   no changes in locomotor activity as denoted by similar average velocity assessment

170   (Supplementary Figure 4A). Moreover, in the EPM test, AP2$\gamma^{+/-}$ mice spent significantly less time

171   in the open-arms than WT mice (Figure 3C). AP2$\gamma^{+/-}$ mice do not show any changes in behavioral

172   despair since immobility times in FST (Figure 3D) and TST (Figure 3E) are identical to WT mice.

173 These observations suggest that anxiety-like behavior promoted by constitutive AP2γ deficiency
174 tend to persist in adult mice, with no alteration in behavioral despair.

175   Cognitive performance assessed by ORT revealed a trend towards a decrease in the
176 preference to explore the displaced object of AP2$\gamma^{+/-}$ when compared to WT mice (p = 0.08, Figure
177 3F). However, no alterations were observed in preference towards the novel object (Figure 3G).
178 In the CFC, a behavior test described to be sensitive to changes in adult hippocampal
179 neurogenesis (Gu et al., 2012), mice were subjected to two distinct context tests, aimed to test
180 hippocampal-dependent memory, and a cue probe to assess the integrity of extrahippocampal
181 memory circuits (Figure 3H) (Gu et al., 2012; Mateus-Pinheiro et al., 2017). In the context A,
182 AP2$\gamma^{+/-}$ mice exhibited reduced freezing behavior when exposed to a familiar context (Figure 3I).
183 No alterations in the freezing behavior were observed neither in the context B (Figure 3J) nor in
184 the cue probe (Figure 3K). These observations suggest that AP2$\gamma^{+/-}$ mice exhibit deficits in
185 contextual hippocampal-related memory, and an intact associative non-hippocampal-dependent
186 memory when compared to WT littermates. Furthermore, experimental groups were also
187 subjected to the MWM test for evaluation of spatial memory (Figure 4). In the reference memory
188 task, that relies on hippocampal function integrity (Cerqueira et al., 2007), AP2$\gamma^{+/-}$ and WT mice
189 exhibit similar performance to reach the hidden platform along the training days (Figure 4A and
190 B). When the platform was changed to the opposite quadrant to assess behavior flexibility, which
191 relies not only in the hippocampal formation but also in prefrontal cortical areas (Hamilton and
192 Brigman, 2015), adult AP2$\gamma^{+/-}$ mice spent less time in the new quadrant than WT animals (Figure
193 4C) suggesting that constitutive AP2γ deficiency leads to impaired behavioral flexibility. Detailed
194 analysis of the strategies adopted to reach the escape platform (Antunes et al., 2020; Garthe et
195 al., 2009; Garthe and Kempermann, 2013; Mateus-Pinheiro et al., 2017; Ruediger et al., 2012)
196 revealed that AP2$\gamma^{+/-}$ mice delayed the switch from non-hippocampal dependent ("Block 1") to
197 hippocampal-dependent ("Block 2") strategies (Figure 4D-H), suggesting an impairment of
198 hippocampal function. No differences were found in the working memory task (Supplementary
199 Figure 4B and C).

200   Overall, results suggest that constitutive heterozygous deletion of AP2γ resulted in specific
201 emotional and cognitive impairments at adulthood. More specifically, we observed that adult
202 AP2$\gamma^{+/-}$ mice display anxiety-like behavior, and cognitive impairments, in contextual memory,
203 spatial memory and behavioral flexibility. Importantly, due to the relevance of hippocampal and
204 mPFC to these behavioral tasks, results suggest that, in adult mice, the functional integrity of
205 these brain areas is highly affected by constitutive and heterozygous deficiency of AP2γ.

206

207

7

208 **Adult hippocampal-to-PFC functional connectivity is disrupted by constitutive AP2γ**

209 **heterozygous deficiency**

210   Given the impact of AP2γ deficiency on emotional and cognitive behavior, we sought for

211 a functional correlate by investigating related neurocircuits. In adult WT and AP2γ$^{+/-}$ mice, we

212 explored the integrity of the dorsal hippocampus (dHip)-to-medial prefrontal cortex (mPFC)

213 circuitry, assessing electrophysiological features of local field potentials (LFPs) simultaneously in

214 these connected brain areas (Figure 5A and Supplementary Figure 5A). In AP2γ$^{+/-}$ mice, the

215 temporal structure of LFPs recorded simultaneously in the dHip and mPFC was affected.

216 Specifically the spectral coherence between these regions (Adhikari et al., 2010; Oliveira et al.,

217 2013; Sardinha et al., 2017) in AP2γ$^{+/-}$ mice is significantly decreased in all frequency bands when

218 compared to WT littermates (Figure 5B), indicating an impaired functional connectivity between

219 these two brain regions in AP2γ$^{+/-}$ mice. While in the dHip, constitutive AP2γ deficiency had a

220 subtle impact in PSD values specifically in the Theta and Beta frequency bands (Figure 5C), in

221 the mPFC, PSD values in all frequencies evaluated were significantly lower than WT mice (Figure

222 5D).

223   Deficiency of AP2γ did not exert an effect neither in the spectral coherence between the

224 vHip and the mPFC (Supplementary Figure 5B) nor in the PSD values in the vHip (Supplementary

225 Figure 5C).

226   The electrophysiological studies revealed that constitutive and heterozygous AP2γ

227 deficiency led to two outcomes: first, a significant decrease of coherence between the dHip and

228 the mPFC indicating impairments in the ability of these regions to functionally interact; second,

229 this decrease in interregional coherence was accompanied by a diminished neuronal activity in a

230 wide range of frequencies in the mPFC, including in theta and beta frequencies, previously shown

231 to be critically related with behavioral outputs dependent on cortico-limbic networks (Colgin, 2011;

232 Fell and Axmacher, 2011; Oliveira et al., 2013).

233

Discussion:

Herein, we show that despite a normal early postnatal acquisition of neurodevelopmental milestones, constitutive and heterozygous deficiency of AP2γ induces an anxiety-like state and causes cognitive deficits in mice that persist from adolescence until adulthood. Our results suggest that AP2γ plays a crucial role for the proper development and maturation of neural circuits implicated in emotional and cognitive functions.

Newly generated neurons are highly relevant to hippocampal functioning and hippocampal-associated behaviors (Anacker and Hen, 2017; Christian et al., 2014; Fang et al., 2018; Gonçalves et al., 2016). Impairments in adult hippocampal neurogenesis precipitate the emergence of depressive- and anxiety-like behaviors (Bessa et al., 2009; Hill et al., 2015; Mateus-Pinheiro et al., 2013b, 2013a; Revest et al., 2009; Sahay and Hen, 2007). Here, we assessed the longitudinal impact of AP2γ, a transcription factor that plays an important role on embryonic neuronal development (Pinto et al., 2009) and recently described as a novel regulator of adult hippocampal neurogenesis (Mateus-Pinheiro et al., 2018, 2017), on neural plasticity, function and behavior at different postnatal periods. Characterization of the neurogenic process in the hippocampal DG in juvenile and adult AP2γ$^{+/-}$ mice, revealed that in agreement with a previous report in a conditional knock-out mice (Mateus-Pinheiro et al., 2017), AP2γ regulates upstream neurogenic regulators as Pax6 and Tbr2. Other modulators of the TAP's population, such as Ngn2 and Tbr2, have been shown to exert a similar control of hippocampal neurogenesis. Ngn2 has been implicated in the proper development of the DG, and its deletion at early stages of development leads to a reduction in neurogenesis (Galichet et al., 2008; Roybon et al., 2009). Moreover, Tbr2 is critically required for hippocampal neurogenesis in the developing and adult mice, with its postnatal inactivation resulting in a marked reduction in neuroblasts (Hodge et al., 2012), and its conditional deletion in the adult hippocampal neurogenic niche leading to a specific blockade of the neurogenic process (Tsai et al., 2015). Also, we observed that, at both postnatal periods, AP2γ plays an essential role in the regulation of pivotal neurogenic steps as NSCs proliferation and neuronal maturation (Mateus-Pinheiro et al., 2017), while the morphology of granular neurons in the hippocampal DG, another form of hippocampal structural plasticity, is intact (Bessa et al., 2009; Mateus-Pinheiro et al., 2013a).

Taking into consideration the embryonic and early postnatal developmental modulatory roles of AP2γ, and the severe and/or lethal malformations during development promoted by deficiencies in other members of the AP2 family (AP2α and AP2β) (Lim et al., 2005; Moser et al., 1997; Schorle et al., 1996), we sought to understand whether constitutive and heterozygous deficiency of AP2γ could lead postnatally to functional and behavioral impairments. The developmental milestones protocol showed no impact of the constitutive heterozygous deficiency of AP2γ in early postnatal neurodevelopment. Nevertheless, this deficiency in AP2γ promotes

9

270 emotional and cognitive behavior in later periods of life. At juvenile age, AP2γ deficiency led to

271 the manifestation of anxiety-like behavior and significant impairments in recognition memory

272 tasks, that depend on the integrity of the hippocampal circuitry (Jessberger et al., 2009).

273 Interestingly, anxiety-like behavior and cognitive impairments were maintained at adulthood,

274 where adult AP2$\gamma^{+/-}$ mice displayed poor performances in hippocampal-dependent tasks (Garthe

275 et al., 2009; Garthe and Kempermann, 2013; Gu et al., 2012; Ruediger et al., 2012). Notably,

276 conditional deletion of AP2γ in adulthood lead to a less evident effect on emotional behavior,

277 namely in anxiety-like behavior tested in the OF and EPM behavioral tests, when comparing with

278 the constitutive mice model herein presented (Mateus-Pinheiro et al., 2017). This result indicates

279 that constitutive deficiency of AP2γ may exert a longitudinal cumulative impact leading to more

280 severe alterations in behavioral performance of mice, whereas in the conditional model during

281 adulthood, the AP2γ deletion only occurs in a subset of newly formed neuroblasts.

282   Our results are consistent with previous publications were the suppression of the TAP's

283 regulator Tbr2 exerted both an anxiety-like phenotype during the juvenile period, and induced

284 cognitive deficits during early adulthood (Veerasammy et al., 2020). Moreover, Ngn2 is also

285 important for the modulation of cognitive behavior, namely in the rescue of cognitive function in

286 the T-Maze task. Interestingly, the regulation of TAPs' by AP2γ seems to be also important for the

287 preservation of cognitive performance as shown by its impact on hippocampal-dependent tasks.

288 Behavioral flexibility, a cognitive task that relies on the interaction of the hippocampal and

289 prefrontal cortical brain areas, was impaired in AP2$\gamma^{+/-}$ mice. Adult AP2$\gamma^{+/-}$ mice present significant

290 deficits of electrophysiological coherence between the dHip and the mPFC. In particular,

291 constitutive AP2γ deficiency led to a decrease of the spectral coherence between the recorded

292 brain areas in a wide range of frequencies, previously associated to behavior outputs dependent

293 on cortico-limbic networks (Colgin, 2011; Fell and Axmacher, 2011; Oliveira et al., 2013; Sardinha

294 et al., 2017). The integrity of the hippocampus-to-PFC circuitry was described to be relevant for

295 example to the action of antidepressants, such as ketamine (Carreno et al., 2016), which promote

296 neurogenesis, suggesting that AP2γ may be involved in conserving this neuronal circuit.

297 Additionally, AP2γ plays an important role on cortical basal progenitors' specification during

298 embryonic development (Pinto et al., 2009) that might be affecting the electrophysiological

299 function of the mPFC. In fact, AP2$\gamma^{+/-}$ mice presented impaired neuronal activity in the mPFC in

300 all frequency ranges, as detected by the general decrease of PSD signals recorded, and

301 corroborated by previous findings (Mateus-Pinheiro et al., 2017). Thus, misspecification of upper

302 cortical layers promoted by AP2γ deficiency since embryonic development may be contributing to

303 the functional electrophysiological readouts, and also eliciting the cognitive defects herein

304 observed.

10

305   Collectively, the results presented in this study demonstrated the importance of the
306   transcription factor AP2γ in the generation of glutamatergic neurons in the postnatal brain and its
307   impact on functional behavioral dimensions at different postnatal periods. Following these
308   findings, future experiments should be implemented to elucidate whether AP2γ can participate in
309   the pathogenesis and treatment of neurodevelopmental and/or psychiatric disorders and how it
310   may exert its modulatory action.
311

312 **Materials and methods:**

313 **Key Resource Table**

Reagent or Resource	Source	Identifier
Experimental model: Organisms/strains		
Mus musculus, mice maintained in a 129/SV background	Dr. Hubert Schorle	NA
Injectables		
BrdU, 50 mg/kg	Sigma-Aldrich	# 9285
Antibodies		
Western blot		
alpha-tubulin, mouse	Sigma	#5168
AP2γ, goat	Abcam	#31288
Pax6, rabbit	Millipore	#2237 RRID:AB_1587367
Sox2, mouse	Abcam	#7935
Anti-mouse	BioRad	#1706516 RRID:AB_11125547
Anti-rabbit	BioRad	#1706515 RRID:AB_11125142
Anti-goat	Santa-Cruz Biotechnologies	#A2216
SuperSignal west Femto reagent	ThermoFisher,	#34096
Immunofluorescence		
BrdU, rat	Abcam	#6326 RRID:AB_305426
Doublecortin, rabbit	Abcam	#18723 RRID:AB_732011
Alexa Fluor 488 Goat Anti-rat	Invitrogen	#32731
Alexa Fluor 568 Goat Anti-rabbit	Invitrogen	#11011 RRID:AB_143157
4',6-diamidino-2-phenylindole (DAPI)	Sigma Aldrich	#8417
Software		
Activity Monitor software	MedAssociates	NA
Kinoscope software	(Kokras et al., 2017)	NA
Ethovision XT 11.5	Noldus	RRID:SCR_000441
Signal Software	CED	NA
Prism v.8	GraphPad Software Inc	RRID:SCR_002798
MATLAB	MathWorks Inc	RRID:SCR_005547

314

315 **Experimental model details:**

316   Wild-type (WT) and AP2γ heterozygous KO (AP2$\gamma^{+/-}$) mice were maintained in a 129/SV

317 background and identified by polymerase chain reaction (PCR) of genomic DNA. Along the study,

318 distinctive at cohorts (at least 2 *per* timepoint) of littermate WT and AP2$\gamma^{+/-}$ male mice were

12

319 submitted to molecular (n = 4-6 *per* group), behavioral (n = 8-16 *per* group) and

320 electrophysiological (n= 5-6 *per* group) assessment at the different postnatal ages (early postnatal

321 period: between postnatal day (PND) 1 and 21; juvenile period: from PND 25 to 31; adulthood:

322 PND 70 to 92).

323   All mice were housed and kept under standard laboratory conditions at 22 ± 1°C, 55%

324 humidity, and *ad libitum* access to food and water on a 12h light/dark cycle (lights on 8 A.M. to 8

325 P.M.). Efforts were made to minimize the number of animals and their suffering. All experimental

326 procedures performed in this work were conducted in accordance with the EU Directive

327 2010/63/EU and approved by the Portuguese National Authority for animal experimentation,

328 *Direção-Geral de Alimentação e Veterinária* (DGAV) with the project reference

329 0420/000/000/2011 (DGAV 4542).

330

331 **Behavioural analysis:**

332 ***Developmental milestones protocol***

333   Early postnatal neurodevelopment in mice was assessed according to previously

334 validated protocols (Castelhano-Carlos et al., 2010; Guerra-Gomes et al., 2020; Hill et al., 2008;

335 Santos et al., 2007). This consisted in a daily evaluation for the first 21 days of life. From postnatal

336 day (PND) 1 onward, newborn animals were evaluated in several parameters, including skin

337 appearance, activity, and presence of milk spot in the stomach, indicator of correct maternal care

338 and well-being. Pups were examined for the acquisition of developmental milestones until

339 weaning (PND21), every day at the same time, in the same experimental room, by the same

340 experimenter. This daily scoring included tests to assess the acquisition of mature response

341 regarding somatic parameters and neurobiological reflexes.

342   *Somatic parameters:*

343   As a measure of morphological development, animals were daily weighed (weight ± 0.01

344 g). The eye-opening day was also evaluated and considered when both eyes were opened. When

345 both eyes opened on different days, score was set as 1 if only one of the eyes was open, and 2

346 when both eyes were open. The mature response was registered when both eyes were open.

347

348   *Neurobiological reflexes:*

349   The assessment of the neurobiological reflexes including the daily performance of

350 different tests. Of note, the scale of evaluation was distinct among tests. Tests including rooting,

351 ear twitch, auditory startle, open field transversal, air righting, wire suspension, postural reflex

352 were scored according to the absence (0) or presence (1) of a mature response. When possible,

353 to detect a gradual progression in performance as for walking, surface righting, grasping, negative

354 geotaxis, cliff aversion, daily score was attributed between 0 and 3, with 0 representing absence,

355 and 3 corresponding to the achievement of the mature response. The postnatal day in which

13

356 animals achieved a mature response was registered. All tests were conducted in a smooth foam

357 pad, and immediately after testing, the pups were returned to their home cage.

358 *Labyrinthine reflex, body righting mechanism, coordination and strength:*

359 *Surface righting reflex* – PND1 to PND13 – This test consists of gently laying the animal

360 on its back, and the mature response was considered when the pup was able to get right. If the

361 animal did not respond within 30 s, the test was ended. Mature response was achieved when the

362 pups were able to get right in less than 1 s for three consecutive days.

363 *Negative geotaxis* – PND1 to PND 14 – Pups were placed head down in a horizontal grid,

364 tilted 45º to the plane. The acquisition of a mature response was set when pups were able to head

365 up in less than 30 s for three consecutive days.

366 *Air righting* – PND8 to PND 21 – In this test, the pup was held upside down and released

367 from a height of approximately 13 cm from the soft padded surface and released. A mature

368 response was obtained when the animals landed on four paws for three consecutive days.

369 *Cliff aversion* – PND 1 to PND 14 – It evaluates the mouse pup's ability to turn and crawl

370 away when on the edge of a cliff. A mature response was achieved once the animal moved away

371 in less than 30 s for three consecutive days.

372 *Postural reflex* – PND 5 to PND 21 – Pups were placed in a small plastic box and gently

373 shaken up down and right. When the animals were able to maintain their original position in the

374 box by extending four paws, mature response was acquired.

375 *Wire suspension* – PND 5 to PND 21 – This test evaluates forelimb grasp and strength.

376 Pups were placed vertically to hold with their forepaws a 3 mm diameter metal wire suspended 5

377 cm above a soft foam pad. A mature response was achieved once the animal was able to grasp

378 the bar, holding it with four paws.

379 *Grasping* – PND 5 to PND 21 – The mouse pup forelimb was stimulated with a thin wire

380 to evaluate when the involuntary freeing reflex stopped. This reflex disappears with the

381 development of the nervous system, as so, the mature response achieved when the animal

382 grasped immediately and firmly the wire.

383

384 *Tactile reflex:*

385 *Ear twitch* – PND 7 to PND 15 – In this test, the mouse pup ear was gently stimulated with

386 the tip of a cotton swab, three times. If the animal reacted, flattening the ear against the side of

387 the head for three consecutive days, the mature response was reached.

388 *Rooting* – PND 7 to PND 12 – A fine filament of a cotton swab was used to gently and

389 slowly rub the animal's head, from the front to the back. It was considered a successful test if the

390 pup moved its head towards the filament. The test was repeated on the other side of the head to

391 evaluate the appearance of this neurobiological reflexes on both sides. If the animal did not react

14

392 to the filament, the test was repeated. Mature response was obtained when animal reacted on

393 both sides for 3 consecutive days.

394

395 *Auditory reflex:*

396   *Auditory startle* – PND7 to PND 18 – We evaluated the reaction of pups to a handclap, at

397 a distance of 10 cm. If pups quick and involuntary jumped for three consecutive days, a matured

398 response was attributed.

399

400 *Motor:*

401   *Open field transversal* – PND7 to PND 18 – To execute this test, animals were placed in

402 a small and circle (13 cm diameter), and time to move was recorded. If the pup was not able to

403 move, the test was ended. In case the mouse leaves the circle in less than 30 s, in three

404 consecutive days, a mature response was reached.

405   *Walking* – PND 5 to PND 21 – In this paradigm, animals were able to freely move around

406 for 60 s. The mature response was achieved when they showed a walking movement fully

407 supported on 4 limbs.

408

409 **Open field (OF) test**

410   The OF test is a behavioral test commonly used to assess anxiety-like behavior,

411 exploratory behavior, and general activity in rodents. This apparatus consists of a highly

412 illuminated square arena of 43.2x43.2cm, closed by a 30.5 cm high wall. Mice were individually

413 placed in the center of the OF arena, and their movement was tracked for 5 mins, using a 16-

414 beam infrared system (MedAssociates, US). Data was analysed using the Activity Monitor

415 software (MedAssociates, US). Average velocity of the animals was considered as a measure of

416 locomotor capacity, and the activity ratio between the center and the arena periphery was

417 considered as measurement of anxiety-like behavior.

418

419 **Elevated-plus maze (EPM) test**

420   To study the impact on anxiety-like behavior the EPM test was also performed (Walf and

421 Frye, 2007). This consists of a black propylene apparatus (ENV – 560; MedAssociates Inc, US)

422 with two opposite open arms (50.8 cm × 10.2 cm) and two closed arms (50.8 cm × 10.2 cm × 40.6

423 cm) elevated 72.4 cm above the floor and dimly illuminated. The central area connecting both

424 arms measured 10x10 cm. Animals were individually positioned in the center of the maze, facing

425 an edge of a closed-arm, and were allowed to freely explore the maze for 5 min. All trials were

426 recorded using an infrared photobeam system, and the percentage of time spent in the open arms

427 was accessed through the EthoVision XT 11.5 tracking system (Ethovision, Noldus Information

428 Technologies, Netherlands).

15

Forced swimming test (FST)

For the assessment of behavioral-despair, we performed the forced swimming test (Porsolt et al., 1977). Briefly, each animal was individually placed in glass cylinders filled with water (23ºC; depth 30 cm) for 5 min. All sessions were video-recorded, and the immobility time, defined through a video tracking software Ethovision XT 11.5 (Noldus, Netherlands), was considered as a measure of learned-helplessness. Mice were considered immobile when all active behaviors (struggling, swimming, and jumping) were ceased. For immobility, the animals had to remain passively floating or making minimal movements need to maintain the nostrils above water. For learned-helplessness assessment, the first 3 min of the trial were considered as a habituation period and the last 2 min as the test period.

Tail-suspension test (TST)

The TST is a commonly used behavioral test to assess behavioral despair in rodents. The principle of this behavioral paradigm is similar to the FST assessing also learned helplessness of the animals. For this, animals were suspended by the tail to the edge of a laboratory bench 80 cm above the floor (using adhesive tape) for 6 min. Trials were video-recorded, and the immobility and climbing times were automatically analyzed by the video tracking software Ethovision XT 11.5 (Noldus, Netherlands). For the learned-helplessness assessment, the first 3 min of the trial was considered as a habituation period, and the last 3 min as the test period.

Splash-sucrose test (SCT)

The splash-sucrose test consists of spraying a 10 %sucrose solution on the dorsal coat of mice in their home cage (Yalcin et al., 2008). Sucrose solution in the mice's coat induces grooming behavior. After spraying the animals, animal was video-recorded for 5 min and the time spent grooming was taken as an index of self-care and motivational behavior. Then, the videos were manually analyzed using the behavioral scoring program Kinoscope (Kokras et al., 2017).

Object recognition test (ORT)

Through this behavioral paradigm we assessed short- and long-term memory (Leger et al., 2013). This test relies on rodents' nature to explore and prefer novelty. For that, mice were acclimatized to a testing arena (30 cm x 30 cm x 30 cm) under dim light for 3 days during 20 min. After habituation, animals were presented with two equal objects for 10 min (training), positioned in the center of the arena. Then, 1 h later, one of the objects was moved towards one arena wall, and mice were allowed to freely explore the objects for 10 mins. On the following day, animals returned to the arena for 10 mins, with one of the objects replaced by a novel object. The familiar and novel objects had different size, color, shape and texture. Between trials, the arena and objects were properly cleaned with 10% ethanol. Sessions were recorded and manually scored

466　through the behavioral scoring program Kinoscope (Kokras et al., 2017). The percentage of time

467　exploring the moved- and novel-object was used as a measure of short- and long-term memory,

468　respectively.

469

470　***Contextual-fear conditioning (CFC)***

471　　　The CFC test was performed in a white acrylic box with internal dimensions of 20 cm wide,

472　16 cm deep, and 20.5 cm high (MedAssociates). This apparatus had a fixed light bulb mounted

473　directly above the chamber to provide a source of illumination. Each box contained a stainless-

474　steel shock grid floor inside a clear acrylic cylinder, where the animals were placed. All animals

475　were exposed to two probes: a context probe and a cue (light) probe, as previously described (Gu

476　et al., 2012; Mateus-Pinheiro et al., 2017). All probes were recorded, and the freezing behavior

477　was manually scored through Kinoscope (Kokras et al., 2017). This behavioral paradigm took 3

478　days.

479　　　Day 1: Animals were individually placed in the conditioning-white box (Context A) and

480　received three pairings between a light (20 s) and a co-terminating shock (1 s, » 0.5 mA). The

481　interval between pairings was 180 s, and the first light presentation started 180 s after the

482　beginning of the trial. After the three pairings, mice remained in the acrylic box for 30 s, being

483　after returned to their home cage. Between animals, the apparatus was properly cleaned with

484　10% ethanol.

485　　　Day 2: For the context probe, animals were placed into the same white acrylic chamber

486　(context A), 24h hours after the light-shock pairings. The freezing behavior was monitored for 3

487　min. Two hours later, we introduced the animals into a modified version of the chamber (Context

488　B). This new box was sheeted with a black plasticized cover, sprayed with a vanilla scent. In this

489　way, both contexts had distinct spatial and odor cues. Also in Context B, the ventilation was not

490　operated, and the experimenter wore a different color of gloves and a lab coat. Freezing behavior

491　was measured for 3 min. The freezing behavior state was defined as the total absence of motion,

492　for a minimum of 1 s.

493　　　Day 3: For the cue probe, the animals were set in Context B, and individually placed in this

494　chamber 24h after the context probe. After 3 min, the light was turned on for 20 s, and the freezing

495　behavior monitored for 1 min after light is turned off.

496

497　***Morris water maze (MWM)***

498　　　In the MWM test, several cognitive domains were assessed: working- and spatial-

499　reference memory and behavioral flexibility. Additionally, the strategies used to reach the platform

500　were also analyzed. MWM was performed in a circular white pool (170 cm diameter) filled with

501　water at 22ºC to a depth of 31 cm in a room with and dim light and extrinsic clues (triangle, square,

502　cross, and horizontal stripes). The pool was divided into four quadrants by imaginary lines, and a

503 clear-acrylic cylinder platform (12 cm diameter; 30 cm high), placed in one of the quadrants. All
504 trials were video recorded by a tracking system (Viewpoint, France).

505

506 *Working memory task:*

507   The working memory task (Alves et al., 2017; Cerqueira et al., 2007) evaluates the
508 cognitive domain that relies on the interplay between the hippocampal and prefrontal cortex (PFC)
509 functions. In this task, animals had to learn the position of the hidden platform and to retain this
510 information for four consecutive daily trials. The task was performed during 4 days and in a
511 clockwise manner the platform was repositioned in a new quadrant each day. During the daily
512 trials, animals had different starting positions (north, east, west, and south). Trials ended when
513 the platform was reached within the time limit of 120 s. If the animals did not reach the platform
514 during the trial time, they were guided to the platform and allowed to stay for 30 s. The time and
515 path to reach the platform were recorded.

516

517 *Reference memory task:*

518   After working memory evaluation (days 1-4), spatial-reference memory, a hippocampal
519 dependent-function, was assessed by keeping the platform in the same quadrant during three
520 consecutive days (days 4-6) (Morris, 1984). The time and path to reach the platform were
521 recorded for each trial.

522

523 *Reversal learning task:*

524   On the last day of MWM testing, reversal-learning performance, a PFC dependent
525 function, was assessed. This was conducted by positioning the platform in a new (opposite)
526 quadrant. Animals were tested in 4 trials. The percentage of time spent in the new and old
527 quadrant containing the platform was used as readout of behavioral flexibility.

528

529 *Search strategies analysis:*

530   Throughout the Morris water maze, animals were evaluated through the adopted
531 strategies to reach the hidden platform, as previously described (Garthe and Kempermann, 2013;
532 Mateus-Pinheiro et al., 2017; Ruediger et al., 2012). Quantitative analyses and strategy
533 classification were completed by assessing different parameters collected through the Viewpoint
534 software: (1) thigmotaxis (Tt): most of the swim distance (>70%) happened within the outer ring
535 area (8 cm from the pool border; (2) random swim (RS): most of the swim distance (>80%)
536 occurred within the inner circular area, and all quadrants were explored with a percentage of swim
537 distance not below 50% for none of the quadrants; non-circular trajectories; (3) scanning (Sc):
538 most of the swim pattern and distance (>80%) happened within the inner circular area, with
539 balanced exploration in all quadrants of the pool; non-circular trajectories, with a percentage

18

540   (<60%) of swim distance in the platform corridor area (area centered along the axis that connects
541   the start position and the hidden platform); (4) chaining (Ch): the majority of the swim distance
542   occurred in the inner circular area (>80%), with a balanced exploration of all pool quadrants; swim
543   distance in the platform corridor area <60%, with circular trajectories taking place; (5) directed
544   search (DS): the majority of the swim distance occurred in the inner circular area (>80%); swim
545   distance in the platform corridor area >60%, with shifts in the trajectories directions; (6) focal
546   search (FS): directed trajectories to the platform zone, with swim exploration within the perimeter
547   of the escape platform (30cm); (7) directed swim (DSw): directed trajectories to the hidden
548   platform, without much exploration of the pool. For simplification, we defined two blocks of
549   strategies: Block 1, that comprises the "non-hippocampal dependent strategies" (Tt, RS, and Sc),
550   and Block 2, comprising the defined "hippocampal dependent strategies" (DS, FS, and DSw).
551   These blocks were defined when a sequence of at least three trials within the same block were
552   reached.
553
554   **Electrophysiological studies**
555   Electrophysiological recordings were obtained from anesthetized mice (sevoflurane
556   2,5%; 800 mL/min). A surgical procedure was performed to insert platinum/iridium concentric
557   electrodes (Science Products) in the target positions following the mouse brain atlas (from
558   Paxinos): prelimbic region of the medial prefrontal cortex (mPFC): 1.94 mm anterior to bregma,
559   0.4 mm lateral to the midline, 2.5 mm below bregma; dorsal hippocampus (dHIP): 1.94 mm
560   posterior to bregma, 1.2 mm lateral to the midline, 1.35 mm below bregma); ventral hippocampus
561   (vHIP): 3.8 mm posterior to bregma, 3.3 mm lateral to the midline, 3.4 mm below bregma). LFP
562   signals obtained from mPFC, dHIP, and vHIP were amplified, filtered (0.1–300 Hz, LP511 Grass
563   Amplifier, Astro-Med), acquired (Micro 1401 mkII, CED) and recorded through the Signal Software
564   (CED). Local field activity was recorded at the sampling rate of 1000 Hz during 100s. After
565   electrophysiological recordings, a biphasic 0.7 mA stimulus was delivered to mark the recording
566   sites. Then, mice were deeply anesthetized with sodium pentobarbital, brains removed, immersed
567   in paraformaldehyde (PFA) 4% for 48h and sectioned (50 μm) in the vibratome. Coronal slices
568   containing the mPFC, dHip vHip were stained for Cresyl Violet to check for recording sites.
569   Animals with recording positions outside at least in one of the two regions under study (mPFC
570   and dHip or vHip) were excluded from the analysis. Coherence analysis was based on multi-taper
571   Fourier analysis.
572   Coherence was calculated by custom-written MATLAB scripts, using the MATLAB
573   toolbox Chronux (http://www.chronux.org) (Mitra and Pesaran, 1999). Coherence was calculated
574   for each 1 s long segments and their mean was evaluated for all frequencies from 1 to 90 Hz. The
575   power spectral density (PSD) of each channel was calculated through the $10 \times \log$ of the
576   multiplication between the complex Fourier Transform of each 1s long data segment and its

577 complex conjugate. The mean PSD of each channel was evaluated for all frequencies from 1 to
578 90 Hz (Oliveira et al., 2013). Both coherence and PSD measurements were assessed in the
579 following frequencies: delta (1–4 Hz), theta (4–12 Hz), beta (12–20 Hz); low (20–40 Hz) and high
580 gamma (40-90 Hz).

581

582 **BrdU labelling**

583 To assess the effect of AP2γ heterozygous deletion on the proliferation of fast-dividing
584 progenitor cells, and its impact on the generation of adult-born neurons, animals from all groups
585 were injected intraperitoneally with the thymidine analogous 5-bromo-2'-deoxyuridine or
586 bromodeoxyuridine (BrdU, 50 mg/kg; Sigma-Aldrich, US) that is incorporated in the DNA during
587 the S-phase. BrdU injections were performed once, at the end of the behavioral assessment, 24
588 h prior to occision.

589

590 **Western Blot analysis**

591 Hippocampal DG of juvenile and adult AP2$\gamma^{+/-}$ mice and WT littermates were carefully
592 macrodissected out after occision. The tissue was weighted and homogenized in RIPA buffer
593 [containing 50mM Tris HCl, 2 mM EDTA, 250 mM NaCl, 10 % glycerol, 1 mM PMSF protease
594 inhibitors (Roche, Switzerland)] and then sonicated (Sonics & Materials, US) for 2 min. Samples
595 were centrifuged for 25 min at 10.000 rpm and 4°C. The protein concentration of the supernatant
596 was determined using Bradford assay. Samples with equal amounts of protein, 30 μg, were
597 analyzed using the following primary antibodies: alpha-tubulin (#5168; Sigma, mouse, 1:5000),
598 AP2γ (#31288; goat, 1:500; Abcam, UK), Pax6 (#2237; rabbit, 1:1000; Millipore, US), Sox2
599 (#7935; mouse, 1:500; Abcam, UK) and Tbr2 (#2283; rabbit, 1:500; Millipore, US). Secondary
600 antibodies were used from BioRad (Anti-mouse, 1:10.000; #1706516; Anti-rabbit, 1:10.000;
601 #1706515, US) and Santa-Cruz Biotechnologies (Anti-goat, 1:7500; #A2216, US). Membranes
602 were developed using SuperSignal west Femto reagent (#34096; ThermoFisher, US) and
603 developed in Sapphire Biomolecular Imager from Azure Biosystems (US). After developing,
604 images were quantified using AzureSpot analysis software (Azure Biosystems, US).

605

606 **Immunostaining procedures**

607 All mice were deeply anesthetized and then transcardially perfused with cold 0.9% NaCl,
608 followed by 4% paraformaldehyde (PFA). Brains were carefully removed from the skull, postfixed
609 in 4% PFA, and then cryoprotected in 30% sucrose solution. The brains were coronally processed
610 at the vibratome (Leica VT 1000S, Germany) with a thickness of 50 mm, extending over the entire
611 length of the hippocampal formation. Coronal sections containing the hippocampal dentate gyrus
612 (DG) were further stained to assess cell proliferation and the population of neuroblasts. For that

613   purpose, brain sections were double stained for BrdU (#6326; rat, 1:100; Abcam, UK) and

614   doublecortin (DCX; #18723; rabbit, 1:100; Abcam, UK). Appropriate secondary fluorescent

615   antibodies were used (Alexa Fluor 488 Goat Anti-rat, #32731; 1:1000; Invitrogen, US; and Alexa

616   Fluor 568 Goat Anti-rabbit, #11011; 1:1000; Invitrogen, US). For Cell nuclei labeling, 4',6-

617   diamidino-2-phenylindole (DAPI, 1:200; Sigma Aldrich) was used. The density of each cell

618   population in the DG was determined by normalizing positive cells with the corresponding area.

619   Analysis and cell counting were performed using a confocal microscope (Olympus FluoViewTM

620   FV1000, Hamburg, Germany) and an optical microscope (Olympus BX51). The observer was

621   blind to the experimental condition of each subject. Data are reported as the number of cells *per*

622   100 μm^2.

623

624   **3D morphological analysis**

625   To evaluate the 3D dendritic morphology of pre-existing granule neurons in the DG we

626   performed impregnation with Golgi-Cox technique in brain sections from juvenile and adult mice.

627   Briefly, brains were immersed in Golgi-Cox solution for 14 days and then transferred to 30%

628   sucrose. Coronal sections (200 μm) were cut on a vibratome (Leica VT100S, Germany), collected

629   and then blotted dry onto gelatine-coated microscope slides. Sections containing the dorsal

630   hippocampus were then alkalinized in 18.8% ammonia, developed in Dektol (Kodak, US), fixed

631   in Kodak Rapid Fix, dehydrated and xylene cleared. Dendritic arborization was analyzed in the

632   DG of WT and AP2$\gamma^{+/-}$ animals (10 neurons *per* animal).

633

634   **Data analysis and statistics**

635   Statistical analysis was performed using Prism v.8 (GraphPad Software, US). Animals

636   were randomly assigned to groups, balanced by genotypes. Sample sizes were determined by

637   power analyses based on previously published studies (Mateus-Pinheiro et al., 2017) and normal

638   distributions were assessed using the Shapiro-Wilk statistical test, taking into account the

639   respective histograms and measures of skewness and kurtosis. To variables that followed the

640   Gaussian distribution within groups, parametric tests were applied, while non-parametric tests

641   were used for discrete variables. To compare the mean values for two groups, a two-tailed

642   independent-sample t-test was applied. For comparisons between two time-points a two-way

643   ANOVA was used. For longitudinal analyses (across days and different trials) a repeated

644   measures ANOVA was used.

645   For the comparison of categorical variables (strength to grab, limb grasping and clasping),

646   crosstabulations were performed and the statistical test used was Fisher's exact test (when

647   Pearson Qui-Squared assumptions were not met).

648   Data is expressed either as mean ± SEM (standard error of the mean), as median, or as

649   percentage, as stated in the figures' legends. Statistical significance was set when $p < 0.05$.

650

651   **Acknowledgments and funding**

664

665   **Author contributions**

666   E.L.C. and N.D.A. maintained the AP2$\gamma^{+/-}$ colony, genotyping and conducted all

667   behavioral tests, molecular and immunohistological analyses. E.L.C. and N.D.A. also completed

668   all the analyses and interpreted the results. P.P. assisted in the occision of the animals and

669   performed the macrodissection of all analyzed brain areas. C.S.C. and J.S assisted in the western

670   blots. A.M.P. helped with cognitive assessment and analyses. E.L.C., N.D.A., C.S.C., and V.M.S.

671   collected and analyzed the electrophysiology results. T.S.R. assisted colony maintenance and

672   genotyping. B.M.P conducted and helped with cognitive assessment and analysis. J.F.O.

673   interpreted the electrophysiological data. E.L.C., N.D.A., and L.P. designed the study, planned

674   the experiments, and wrote the manuscript. E.L.C., N.D.A., A.J.R., J.F.O., N.S. and L.P. edited

675   the manuscript.

676

677   **Competing interests**

678   The authors declare that they have no competing interests.

679

680

References

Adhikari A, Topiwala MA, Gordon JA. 2010. Synchronized Activity between the Ventral Hippocampus and the Medial Prefrontal Cortex during Anxiety. *Neuron* **65**:257–269. doi:10.1016/j.neuron.2009.12.002

Alves ND, Correia JS, Patrício P, Mateus-Pinheiro A, Machado-Santos AR, Loureiro-Campos E, Morais M, Bessa JM, Sousa N, Pinto L. 2017. Adult hippocampal neuroplasticity triggers susceptibility to recurrent depression. *Transl Psychiatry* **7**:e1058–e1058. doi:10.1038/tp.2017.29

Anacker C, Hen R. 2017. Adult hippocampal neurogenesis and cognitive flexibility — linking memory and mood. *Nat Rev Neurosci* **18**:335–346. doi:10.1038/nrn.2017.45

Antunes C, Da Silva JD, Guerra-Gomes S, Alves ND, Ferreira F, Loureiro-Campos E, Branco MR, Sousa N, Reik W, Pinto L, Marques CJ. 2020. Tet3 ablation in adult brain neurons increases anxiety-like behavior and regulates cognitive function in mice. *Mol Psychiatry*. doi:10.1038/s41380-020-0695-7

Bertrand N, Castro DS, Guillemot F. 2002. Proneural genes and the specification of neural cell types. *Nat Rev Neurosci* **3**:517–530. doi:10.1038/nrn874

Bessa JM, Ferreira D, Melo I, Marques F, Cerqueira JJ, Palha JA, Almeida OFX, Sousa N. 2009. The mood-improving actions of antidepressants do not depend on neurogenesis but are associated with neuronal remodeling. *Mol Psychiatry* **14**:764–773. doi:10.1038/mp.2008.119

Boldrini M, Fulmore CA, Tartt AN, Simeon LR, Pavlova I, Poposka V, Rosoklija GB, Stankov A, Arango V, Dwork AJ, Hen R, Mann JJ. 2018. Human Hippocampal Neurogenesis Persists throughout Aging. *Cell Stem Cell* **22**:589-599.e5. doi:10.1016/j.stem.2018.03.015

Brill MS, Ninkovic J, Winpenny E, Hodge RD, Ozen I, Yang R, Lepier A, Gascón S, Erdelyi F, Szabo G, Parras C, Guillemot F, Frotscher M, Berninger B, Hevner RF, Raineteau O, Götz M. 2009. Adult generation of glutamatergic olfactory bulb interneurons. *Nat Neurosci* **12**:1524–1533. doi:10.1038/nn.2416

Carreno FR, Donegan JJ, Boley AM, Shah A, DeGuzman M, Frazer A, Lodge DJ. 2016. Activation of a ventral hippocampus–medial prefrontal cortex pathway is both necessary and sufficient for an antidepressant response to ketamine. *Mol Psychiatry* **21**:1298–1308. doi:10.1038/mp.2015.176

Castelhano-Carlos MJ, Sousa N, Ohl F, Baumans V. 2010. Identification methods in newborn C57BL/6 mice: a developmental and behavioural evaluation. *Lab Anim* **44**:88–103. doi:10.1258/la.2009.009044

Cerqueira JJ, Mailliet F, Almeida OFX, Jay TM, Sousa N. 2007. The Prefrontal Cortex as a Key Target of the Maladaptive Response to Stress. *J Neurosci* **27**:2781–2787. doi:10.1523/JNEUROSCI.4372-06.2007

718   Christian KM, Song H, Ming G. 2014. Functions and Dysfunctions of Adult Hippocampal
719   Neurogenesis. *Annu Rev Neurosci* **37**:243–262. doi:10.1146/annurev-neuro-071013-
720   014134

721   Colgin LL. 2011. Oscillations and hippocampal–prefrontal synchrony. *Curr Opin Neurobiol*
722   **21**:467–474. doi:10.1016/j.conb.2011.04.006

723   Dennis C V., Suh LS, Rodriguez ML, Kril JJ, Sutherland GT. 2016. Human adult neurogenesis
724   across the ages: An immunohistochemical study. *Neuropathol Appl Neurobiol* **42**:621–
725   638. doi:10.1111/nan.12337

726   Eckert D, Buhl S, Weber S, Jäger R, Schorle H. 2005. The AP-2 family of transcription factors.
727   *Genome Biol*. doi:10.1186/gb-2005-6-13-246

728   Englund C. 2005. Pax6, Tbr2, and Tbr1 Are Expressed Sequentially by Radial Glia, Intermediate
729   Progenitor Cells, and Postmitotic Neurons in Developing Neocortex. *J Neurosci* **25**:247–
730   251. doi:10.1523/JNEUROSCI.2899-04.2005

731   Fang J, Demic S, Cheng S. 2018. The reduction of adult neurogenesis in depression impairs the
732   retrieval of new as well as remote episodic memory. *PLoS One* **13**:e0198406.
733   doi:10.1371/journal.pone.0198406

734   Fell J, Axmacher N. 2011. The role of phase synchronization in memory processes. *Nat Rev*
735   *Neurosci* **12**:105–118. doi:10.1038/nrn2979

736   Galichet C, Guillemot F, Parras CM. 2008. Neurogenin 2 has an essential role in development
737   of the dentate gyrus. *Development* **135**:2031–2041. doi:10.1242/dev.015115

738   Garthe A, Behr J, Kempermann G. 2009. Adult-Generated Hippocampal Neurons Allow the
739   Flexible Use of Spatially Precise Learning Strategies. *PLoS One* **4**:e5464.
740   doi:10.1371/journal.pone.0005464

741   Garthe A, Kempermann G. 2013. An old test for new neurons: refining the Morris water maze to
742   study the functional relevance of adult hippocampal neurogenesis. *Front Neurosci* **7**.
743   doi:10.3389/fnins.2013.00063

744   Geneviève D, Sanlaville D, Faivre L, Kottler M-L, Jambou M, Gosset P, Boustani-Samara D,
745   Pinto G, Ozilou C, Abeguilé G, Munnich A, Romana S, Raoul O, Cormier-Daire V,
746   Vekemans M. 2005. Paternal deletion of the GNAS imprinted locus (including Gnasxl) in
747   two girls presenting with severe pre- and post-natal growth retardation and intractable
748   feeding difficulties. *Eur J Hum Genet* **13**:1033–1039. doi:10.1038/sj.ejhg.5201448

749   Gonçalves JT, Schafer ST, Gage FH. 2016. Adult Neurogenesis in the Hippocampus: From Stem
750   Cells to Behavior. *Cell* **167**:897–914. doi:10.1016/j.cell.2016.10.021

751   Götz M, Stoykova A, Gruss P. 1998. Pax6 Controls Radial Glia Differentiation in the Cerebral
752   Cortex. *Neuron* **21**:1031–1044. doi:10.1016/S0896-6273(00)80621-2

753   Gu Y, Arruda-Carvalho M, Wang J, Janoschka SR, Josselyn SA, Frankland PW, Ge S. 2012.
754   Optical controlling reveals time-dependent roles for adult-born dentate granule cells. *Nat*

755   *Neurosci*. doi:10.1038/nn.3260

756   Guerra-Gomes S, Cunha-Garcia D, Marques Nascimento DS, Duarte-Silva S, Loureiro-Campos
757   E, Morais Sardinha V, Viana JF, Sousa N, Maciel P, Pinto L, Oliveira JF. 2020. IP3R2 null
758   mice display a normal acquisition of somatic and neurological development milestones.
759   *Eur J Neurosci*. doi:10.1111/ejn.14724

760   Hack MA, Saghatelyan A, de Chevigny A, Pfeifer A, Ashery-Padan R, Lledo P-M, Götz M. 2005.
761   Neuronal fate determinants of adult olfactory bulb neurogenesis. *Nat Neurosci* **8**:865–872.
762   doi:10.1038/nn1479

763   Hamilton DA, Brigman JL. 2015. Behavioral flexibility in rats and mice: Contributions of distinct
764   frontocortical regions. *Genes, Brain Behav*. doi:10.1111/gbb.12191

765   Hevner RF. 2019. Intermediate progenitors and Tbr2 in cortical development. *J Anat* **235**:616–
766   625. doi:10.1111/joa.12939

767   Hevner RF, Hodge RD, Daza RAM, Englund C. 2006. Transcription factors in glutamatergic
768   neurogenesis: Conserved programs in neocortex, cerebellum, and adult hippocampus.
769   *Neurosci Res* **55**:223–233. doi:10.1016/j.neures.2006.03.004

770   Heyser CJ. 2003. Assessment of Developmental Milestones in Rodents. *Curr Protoc Neurosci*
771   **25**. doi:10.1002/0471142301.ns0818s25

772   Hilger-Eversheim K, Moser M, Schorle H, Buettner R. 2000. Regulatory roles of AP-2
773   transcription factors in vertebrate development, apoptosis and cell-cycle control. *Gene*
774   **260**:1–12. doi:10.1016/S0378-1119(00)00454-6

775   Hill AS, Sahay A, Hen R. 2015. Increasing Adult Hippocampal Neurogenesis is Sufficient to
776   Reduce Anxiety and Depression-Like Behaviors. *Neuropsychopharmacology* **40**:2368–
777   2378. doi:10.1038/npp.2015.85

778   Hill JM, Lim MA, Stone MM. 2008. Developmental Milestones in the Newborn Mouse. pp. 131–
779   149. doi:10.1007/978-1-60327-099-1_10

780   Hochgerner H, Zeisel A, Lönnerberg P, Linnarsson S. 2018. Conserved properties of dentate
781   gyrus neurogenesis across postnatal development revealed by single-cell RNA
782   sequencing. *Nat Neurosci* **21**:290–299. doi:10.1038/s41593-017-0056-2

783   Hodge RD, Nelson BR, Kahoud RJ, Yang R, Mussar KE, Reiner SL, Hevner RF. 2012. Tbr2 Is
784   Essential for Hippocampal Lineage Progression from Neural Stem Cells to Intermediate
785   Progenitors and Neurons. *J Neurosci* **32**:6275–6287. doi:10.1523/JNEUROSCI.0532-
786   12.2012

787   Hoei-Hansen CE, Nielsen JE, Almstrup K, Sonne SB, Graem N, Skakkebaek NE, Leffers H,
788   Rajpert-De Meyts E. 2004. Transcription factor AP-2γ is a developmentally regulated
789   marker of testicular carcinoma in situ and germ cell tumors. *Clin Cancer Res* **10**:8521–
790   8530. doi:10.1158/1078-0432.CCR-04-1285

791   Hsieh J. 2012. Orchestrating transcriptional control of adult neurogenesis. *Genes Dev* **26**:1010–

792   1021. doi:10.1101/gad.187336.112

793 Jessberger S, Clark RE, Broadbent NJ, Clemenson GD, Consiglio A, Lie DC, Squire LR, Gage
794   FH. 2009. Dentate gyrus-specific knockdown of adult neurogenesis impairs spatial and
795   object recognition memory in adult rats. *Learn Mem* **16**:147–154. doi:10.1101/lm.1172609

796 Kase Y, Kase Y, Shimazaki T, Okano H. 2020. Current understanding of adult neurogenesis in
797   the mammalian brain: How does adult neurogenesis decrease with age? *Inflamm Regen*.
798   doi:10.1186/s41232-020-00122-x

799 Katsimpardi L, Lledo PM. 2018. Regulation of neurogenesis in the adult and aging brain. *Curr*
800   *Opin Neurobiol*. doi:10.1016/j.conb.2018.07.006

801 Kempermann G, Gage FH, Aigner L, Song H, Curtis MA, Thuret S, Kuhn HG, Jessberger S,
802   Frankland PW, Cameron HA, Gould E, Hen R, Abrous DN, Toni N, Schinder AF, Zhao X,
803   Lucassen PJ, Frisén J. 2018. Human Adult Neurogenesis: Evidence and Remaining
804   Questions. *Cell Stem Cell* **23**:25–30. doi:10.1016/j.stem.2018.04.004

805 Kempermann G, Jessberger S, Steiner B, Kronenberg G. 2004. Milestones of neuronal
806   development in the adult hippocampus. *Trends Neurosci* **27**:447–452.
807   doi:10.1016/j.tins.2004.05.013

808 Kokras N, Baltas D, Theocharis F, Dalla C. 2017. Kinoscope: An Open-Source Computer
809   Program for Behavioral Pharmacologists. *Front Behav Neurosci* **11**:1–7.
810   doi:10.3389/fnbeh.2017.00088

811 Leger M, Quiedeville A, Bouet V, Haelewyn B, Boulouard M, Schumann-Bard P, Freret T. 2013.
812   Object recognition test in mice. *Nat Protoc*. doi:10.1038/nprot.2013.155

813 Li M, Wang Y, Yu Y, Nishizawa M, Nakajima T, Ito S, Kannan P. 2002. The human transcription
814   factor activation protein-2 gamma (AP-2γ): gene structure, promoter, and expression in
815   mammary carcinoma cell lines. *Gene* **301**:43–51. doi:10.1016/S0378-1119(02)01057-0

816 Lim JH, Booker AB, Luo T, Williams T, Furuta Y, Lagutin O, Oliver G, Sargent TD, Fallon JR.
817   2005. AP-2α selectively regulates fragile X mental retardation-1 gene transcription during
818   embryonic development. *Hum Mol Genet* **14**:2027–2034. doi:10.1093/hmg/ddi207

819 Mateus-Pinheiro A, Alves ND, Patrício P, Machado-Santos AR, Loureiro-Campos E, Silva JM,
820   Sardinha VM, Reis J, Schorle H, Oliveira JF, Ninkovic J, Sousa N, Pinto L. 2017. AP2γ
821   controls adult hippocampal neurogenesis and modulates cognitive, but not anxiety or
822   depressive-like behavior. *Mol Psychiatry* **22**:1725–1734. doi:10.1038/mp.2016.169

823 Mateus-Pinheiro A, Alves ND, Sousa N, Pinto L. 2018. AP2γ: A New Player on Adult
824   Hippocampal Neurogenesis Regulation. *J Exp Neurosci* **12**:1–4.
825   doi:10.1177/1179069518766897

826 Mateus-Pinheiro A, Patrício P, Bessa JM, Sousa N, Pinto L. 2013a. Cell genesis and dendritic
827   plasticity: a neuroplastic pas de deux in the onset and remission from depression. *Mol*
828   *Psychiatry* **18**:748–750. doi:10.1038/mp.2013.56

829   Mateus-Pinheiro A, Pinto L, Bessa JM, Morais M, Alves ND, Monteiro S, Patrício P, Almeida
830   OFX, Sousa N. 2013b. Sustained remission from depressive-like behavior depends on
831   hippocampal neurogenesis. *Transl Psychiatry* **3**:e210–e210. doi:10.1038/tp.2012.141

832   Mitra PP, Pesaran B. 1999. Analysis of Dynamic Brain Imaging Data. *Biophys J* **76**:691–708.
833   doi:10.1016/S0006-3495(99)77236-X

834   Moreno-Jiménez EP, Flor-García M, Terreros-Roncal J, Rábano A, Cafini F, Pallas-Bazarra N,
835   Ávila J, Llorens-Martín M. 2019. Adult hippocampal neurogenesis is abundant in
836   neurologically healthy subjects and drops sharply in patients with Alzheimer's disease.
837   *Nat Med* **25**:554–560. doi:10.1038/s41591-019-0375-9

838   Morris R. 1984. Developments of a water-maze procedure for studying spatial learning in the rat.
839   *J Neurosci Methods* **11**:47–60. doi:10.1016/0165-0270(84)90007-4

840   Moser M, Pscherer A, Roth C, Becker J, Mucher G, Zerres K, Dixkens C, Weis J, Guay-Woodford
841   L, Buettner R, Fassler R. 1997. Enhanced apoptotic cell death of renal epithelial cells in
842   mice lacking transcription factor AP-2beta. *Genes Dev* **11**:1938–1948.
843   doi:10.1101/gad.11.15.1938

844   Nacher J, Varea E, Blasco-Ibañez JM, Castillo-Gomez E, Crespo C, Martinez-Guijarro FJ,
845   McEwen BS. 2005. Expression of the transcription factor Pax6 in the adult rat dentate
846   gyrus. *J Neurosci Res* **81**:753–761. doi:10.1002/jnr.20596

847   Ødegaard E, Staff AC, Kærn J, Flørenes VA, Kopolovic J, Tropé CG, Abeler VM, Reich R,
848   Davidson B. 2006. The AP-2γ transcription factor is upregulated in advanced-stage
849   ovarian carcinoma. *Gynecol Oncol* **100**:462–468. doi:10.1016/j.ygyno.2005.09.022

850   Oliveira JF, Dias NS, Correia M, Gama-Pereira F, Sardinha VM, Lima A, Oliveira AF, Jacinto LR,
851   Ferreira DS, Silva AM, Reis JS, Cerqueira JJ, Sousa N. 2013. Chronic stress disrupts
852   neural coherence between cortico-limbic structures. *Front Neural Circuits* **7**.
853   doi:10.3389/fncir.2013.00010

854   Pinto L, Drechsel D, Schmid M-T, Ninkovic J, Irmler M, Brill MS, Restani L, Gianfranceschi L,
855   Cerri C, Weber SN, Tarabykin V, Baer K, Guillemot F, Beckers J, Zecevic N, Dehay C,
856   Caleo M, Schorle H, Götz M. 2009. AP2γ regulates basal progenitor fate in a region- and
857   layer-specific manner in the developing cortex. *Nat Neurosci* **12**:1229–1237.
858   doi:10.1038/nn.2399

859   Porsolt RD, Bertin A, Jalfre M. 1977. Behavioral despair in mice: a primary screening test for
860   antidepressants. *Arch Int Pharmacodyn Ther* **229**:327–36.

861   Revest J-M, Dupret D, Koehl M, Funk-Reiter C, Grosjean N, Piazza P-V, Abrous DN. 2009. Adult
862   hippocampal neurogenesis is involved in anxiety-related behaviors. *Mol Psychiatry*
863   **14**:959–967. doi:10.1038/mp.2009.15

864   Roybon L, Hjalt T, Stott S, Guillemot F, Li J-Y, Brundin P. 2009. Neurogenin2 Directs Granule
865   Neuroblast Production and Amplification while NeuroD1 Specifies Neuronal Fate during

866   Hippocampal Neurogenesis. *PLoS One* **4**:e4779. doi:10.1371/journal.pone.0004779

867   Ruediger S, Spirig D, Donato F, Caroni P. 2012. Goal-oriented searching mediated by ventral
868   hippocampus early in trial-and-error learning. *Nat Neurosci* **15**:1563–1571.
869   doi:10.1038/nn.3224

870   Sahay A, Hen R. 2007. Adult hippocampal neurogenesis in depression. *Nat Neurosci* **10**:1110–
871   1115. doi:10.1038/nn1969

872   Santos M, Silva-Fernandes A, Oliveira P, Sousa N, Maciel P. 2007. Evidence for abnormal early
873   development in a mouse model of Rett syndrome. *Genes, Brain Behav* **6**:277–286.
874   doi:10.1111/j.1601-183X.2006.00258.x

875   Sardinha VM, Guerra-Gomes S, Caetano I, Tavares G, Martins M, Reis JS, Correia JS, Teixeira-
876   Castro A, Pinto L, Sousa N, Oliveira JF. 2017. Astrocytic signaling supports hippocampal-
877   prefrontal theta synchronization and cognitive function. *Glia* **65**:1944–1960.
878   doi:10.1002/glia.23205

879   Schorle H, Meier P, Buchert M, Jaenisch R, Mitchell PJ. 1996. Transcription factor AP-2 essential
880   for cranial closure and craniofacial development. *Nature* **381**:235–238.
881   doi:10.1038/381235a0

882   Thewes V, Orso F, Jäger R, Eckert D, Schäfer S, Kirfel G, Garbe S, Taverna D, Schorle H. 2010.
883   Interference with Activator Protein-2 transcription factors leads to induction of apoptosis
884   and an increase in chemo- and radiation-sensitivity in breast cancer cells. *BMC Cancer*
885   **10**:192. doi:10.1186/1471-2407-10-192

886   Tobin MK, Musaraca K, Disouky A, Shetti A, Bheri A, Honer WG, Kim N, Dawe RJ, Bennett DA,
887   Arfanakis K, Lazarov O. 2019. Human Hippocampal Neurogenesis Persists in Aged Adults
888   and Alzheimer's Disease Patients. *Cell Stem Cell* **24**:974-982.e3.
889   doi:10.1016/j.stem.2019.05.003

890   Toda T, Parylak SL, Linker SB, Gage FH. 2019. The role of adult hippocampal neurogenesis in
891   brain health and disease. *Mol Psychiatry* **24**:67–87. doi:10.1038/s41380-018-0036-2

892   Tsai Cheng Yu, Tsai Ching Yen, Arnold SJ, Huang GJ. 2015. Ablation of hippocampal
893   neurogenesis in mice impairs the response to stress during the dark cycle. *Nat Commun*
894   **6**:1–7. doi:10.1038/ncomms9373

895   Veerasammy S, Van Steenwinckel J, Le Charpentier T, Seo JH, Fleiss B, Gressens P, Levison
896   SW. 2020. Perinatal IL-1β-induced inflammation suppresses Tbr2+ intermediate
897   progenitor cell proliferation in the developing hippocampus accompanied by long-term
898   behavioral deficits. *Brain, Behav Immun - Heal* **7**:100106. doi:10.1016/j.bbih.2020.100106

899   Waclaw RR, Allen ZJ, Bell SM, Erdélyi F, Szabó G, Potter SS, Campbell K. 2006. The Zinc
900   Finger Transcription Factor Sp8 Regulates the Generation and Diversity of Olfactory Bulb
901   Interneurons. *Neuron* **49**:503–516. doi:10.1016/j.neuron.2006.01.018

902   Walf AA, Frye CA. 2007. The use of the elevated plus maze as an assay of anxiety-related

903   behavior in rodents. *Nat Protoc* **2**:322–328. doi:10.1038/nprot.2007.44

904 Yalcin I, Belzung C, Surget A. 2008. Mouse strain differences in the unpredictable chronic mild

905   stress: a four-antidepressant survey. *Behav Brain Res* **193**:140–143.

906   doi:10.1016/j.bbr.2008.04.021

907

908

909 **Table:**

910 **Table 1:** Results from the milestones protocol tests included in the assessment of early postnatal

911 neurodevelopment. Sample size: n_{WT} = 9; $n_{AP2\gamma}^{+/-}$ = 9. Abbreviations: WT, wild-type; AP2$\gamma^{+/-}$, AP2γ

912 heterozygous mice; PND: Postnatal day

913

| Milestone test	WT Day (median)	AP2$\gamma^{+/-}$ Day (median)	Statistical test, significance Mann-Whitney test	typical range
Rooting (S. Figure 2B)	7	7	U = 31.50, p = 0.43	PND 1 – PND 15
Ear twitch (S. Figure 2C)	8	9	U = 20.50, p = 0.23	PND 6 – PND 14
Auditory startle (S. Figure 2D)	7.5	7	U = 29, p = 0.90	PND 7 – PND 16
Open field (S. Figure 2E)	8	8	U = 27.5, p = 0.73	PND 6 – PND15
Walking (S. Figure 2F)	10	9	U = 33, p = 0.78	PND 7 – PND 14
Surface righting (S. Figure 2G)	6	7	U = 37, p = 0.12	PND1 – PND10
Negative geotaxis (S. Figure 2H)	8	9	U = 25, p = 0.17	PND 3 – PND 15
Cliff aversion (S. Figure 2I)	7.5	6	U = 18; p = 0.26	PND 1 – PND 14
Postural reflex (S. Figure 2J)	9.5	8	U = 23, p = 0.24	PND 5 – PND 21
Air righting (S. Figure 2K)	12	11	U = 29, p = 0.32	PND7 – PND16
Wire suspension (S. Figure 2L)	13	11	U = 21.5, p=0.10	PND 5 – PND 21
Grasping (S. Figure 2M)	16.5	16	U = 25.5, p=0.32	PND 13 - PND17
Eye-opening (S. Figure 2P)	12	11	U = 7.5, p < 0.01	PND 7 - 17
	WT Mean ± SEM	**AP2$\gamma^{+/-}$** Mean ± SEM	**Statistical test, significance** Repeated measures ANOVA	
Homing (S. Figure 2N) — **Trial 1**	6.89 s ± 0.44	6.89 s ± 1.32		
Trial 2	6.33 s ± 1.12	6.89 s ± 1.12	$F_{(1,16)}$ = 0.06, p = 0.80	
Trial 3	5.22 s ± 1 .57	5.78 s ± 1.57		
Weight gain pattern (S. Figure 2O)	8.99 g ± 0.53	9.22 g ± 0.16	$F_{(1,16)}$ = 0.32, p = 0.58	
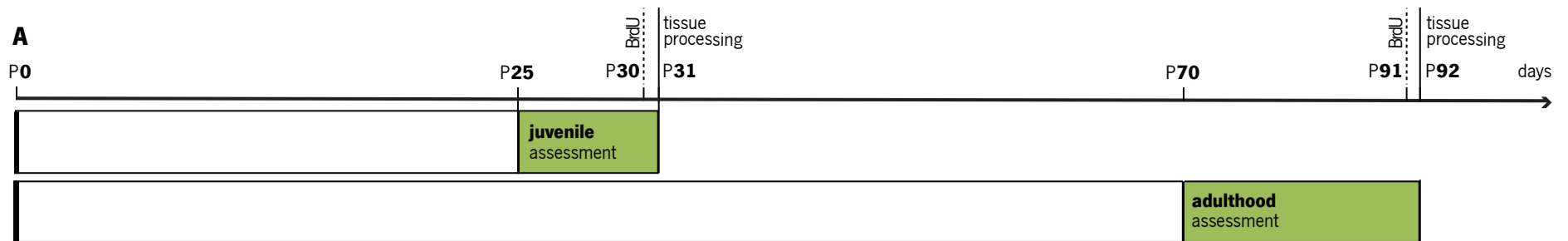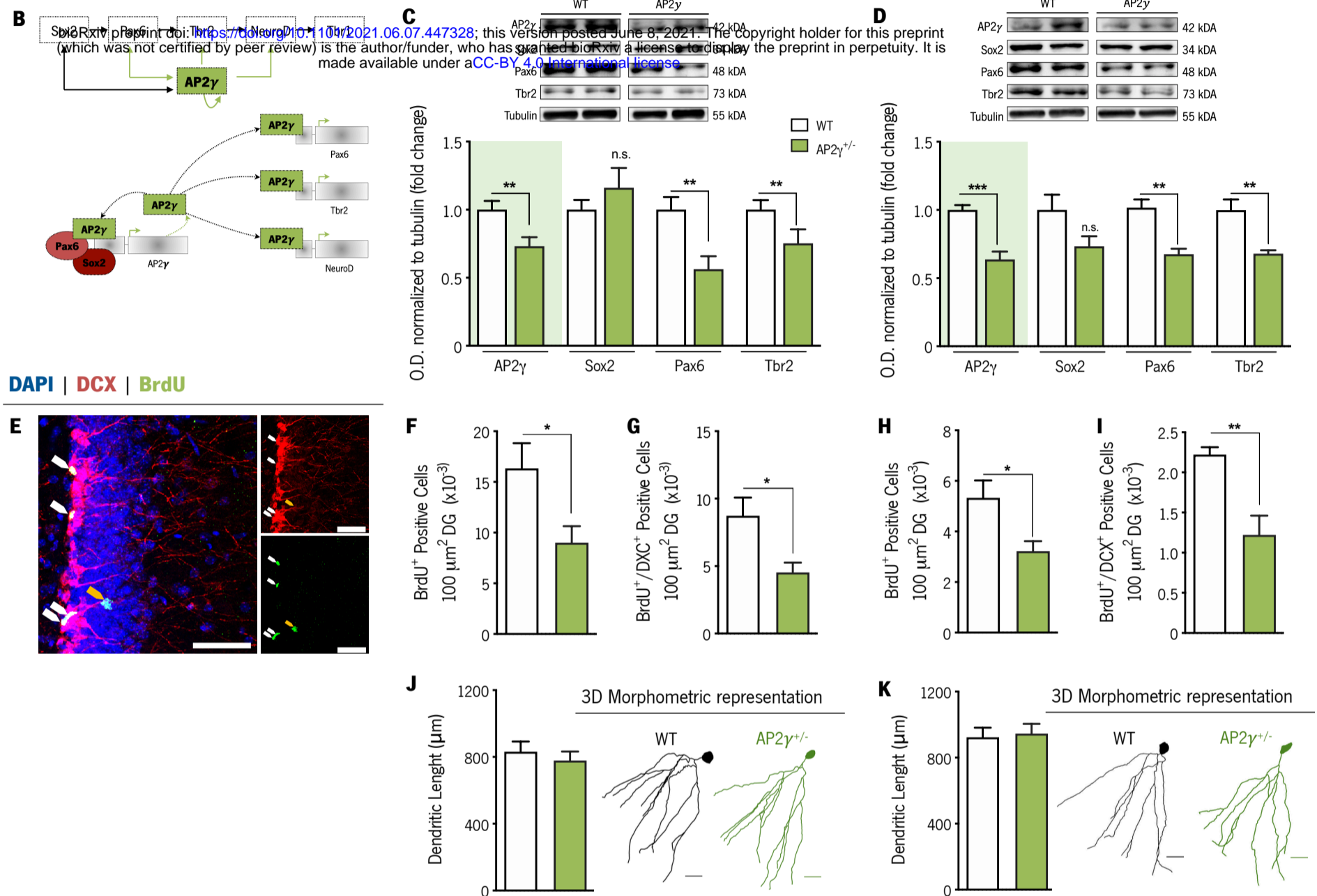
Figure 1: Constitutive and heterozygous AP2γ deficiency reduces postnatal hippocampal neurogenesis both at juvenile and adult periods.

(A) Experimental timeline. (B) Transcriptional network of hippocampal neurogenesis under modulatory role of AP2γ. Western-blot analysis of AP2γ, Sox2, Pax6, and Tbr2 in juvenile (C) and adult (D) dentate gyrus (DG) protein extracts. (E) Hippocampal DG coronal section immunostained for bromodeoxyuridine (BrdU) (green), doublecortin (DCX) (in red), and DAPI (in blue). BrdU/DCX double-positive cells are indicated by white arrows and solely BrdU-positive cell is identified with a yellow arrow. (F-I) Cell counts of BrdU-positive and BrdU/DCX double-positive cells in the hippocampal DG of juvenile and adult mice. (J and K) Dendritic length of three-dimensional (3D) neuronal reconstructed hippocampal granular neurons in juvenile (J) and adult (K) mice. Data presented as mean SEM. Sample size: Western-blot analysis: $n_{WT\ juvenile} = 4$; $n_{AP2\gamma^{+/-}\ juvenile} = 4$; $n_{WT\ adult} = 4$; $n_{AP2\gamma^{+/-}\ adult} = 4$; Immunostainings assays: $n_{WT\ juvenile} = 6$; $n_{AP2\gamma^{+/-}\ juvenile} = 6$; $n_{WT\ adult} = 5$; $n_{AP2\gamma^{+/-}\ adult} = 5$; 3D neuronal reconstruction: $n_{WT\ juvenile} = 4$; $n_{AP2\gamma^{+/-}\ juvenile} = 4$; $n_{WT\ adult} = 4$; $n_{AP2\gamma^{+/-}\ adult} = 5$. [Student's t-test; ***$p<0.001$, ** $p< 0.01$; * $p< 0.05$; Statistical summary in Supplementary table 1]. Scale bars represent 50 m. Abbreviations: WT, wild-type; AP2γ$^{+/-}$, AP2γ heterozygous knockout mice; O.D., optical density.
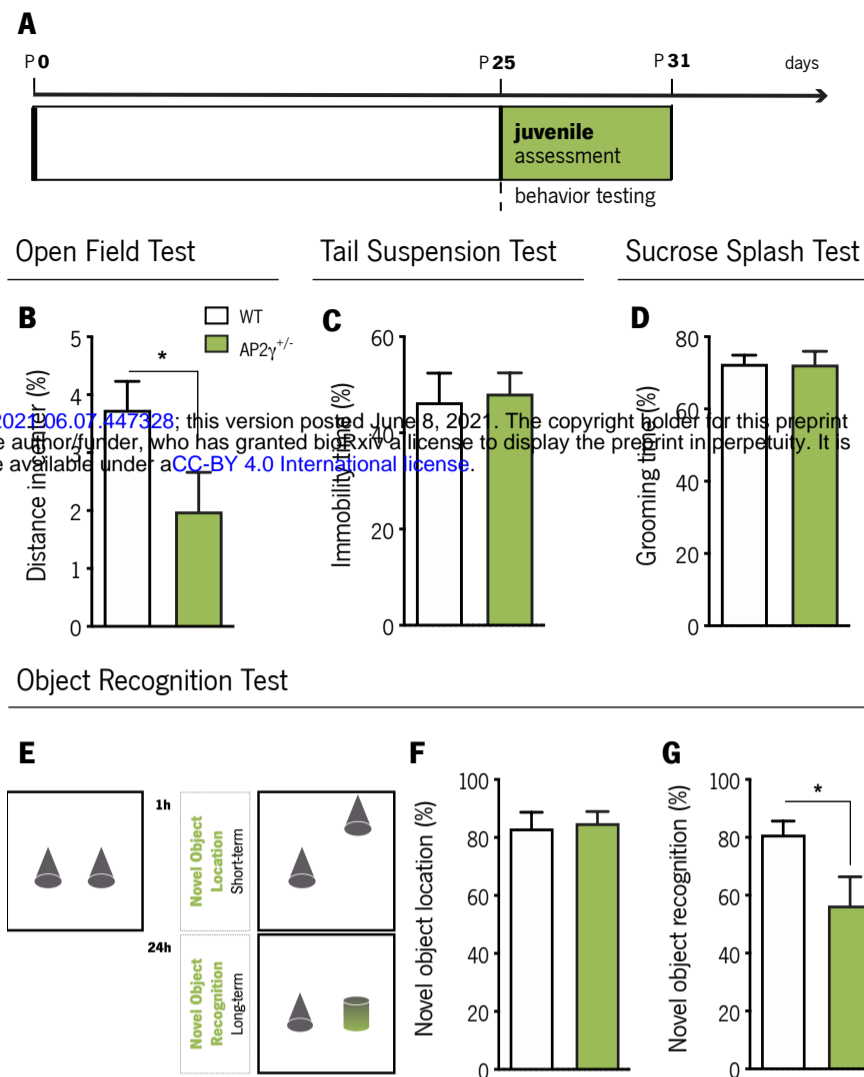
Figure 2: AP2γ deficiency increased anxiety-like behavior and promotes cognitive deficits in juvenile mice. (A) Timeline of behavioral assessment. Anxiety-like behavior was assessed through the open-field test (OF) (B), and depressive- and anhedonic-like behavior by the tail-suspension (TST) (C) and the sucrose splash (SST) (D) test. (E) To evaluate cognition, juvenile mice were subjected to the object recognition test, in particular to the novel object location (F) and the novel object recognition (G) tasks. Data presented as mean SEM. Sample size: OF: n_{WT} = 13; $n_{AP2\gamma}^{+/-}$ = 11; TST: n_{WT} = 16; $n_{AP2\gamma}^{+/-}$ = 13; ST: n_{WT} = 15; $n_{AP2\gamma}^{+/-}$ = 10; ORT: n_{WT} = 11; $n_{AP2\gamma}^{+/-}$ = 8. [Student's t-test; * p< 0.05; Statistical summary in Supplementary table 1]. Abbreviations: WT, wild-type; AP2γ$^{+/-}$, AP2γ heterozygous knockout mice.
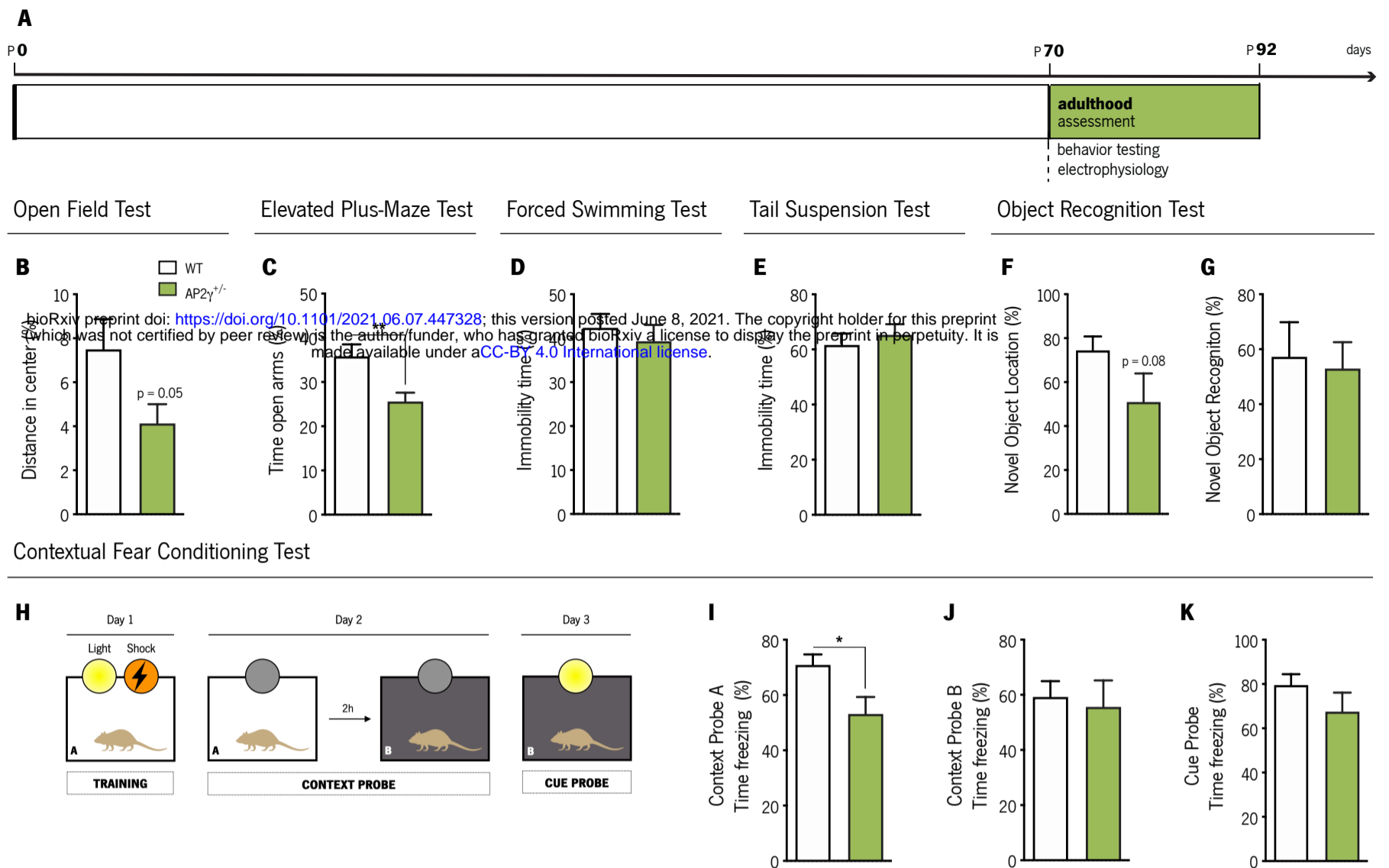
Figure 3: Behavioral assessment of adult mice. (A) Experimental timeline. (B and C) Anxiety-like behavior was assessed through the open-field test (OF) (B) and the elevated plus-maze (EPM) (C), while depressive-like behavior was evaluated through the forced-swimming test (FST) (D) and the tail-suspension (TST) (E) test. Object recognition test (ORT) (F and G) and (H-K) contextual fear conditioning (CFC) were performed to assess cognitive performance. Data presented as mean ± SEM. Sample size: OF, EPM and FST: n_{WT} = 12; $n_{AP2\gamma}^{+/-}$ = 14; TST: n_{WT} = 6; $n_{AP2\gamma}^{+/-}$ = 6; ORT: n_{WT} = 12; $n_{AP2\gamma}^{+/-}$ = 9; CFC: n_{WT} = 7; $n_{AP2\gamma}^{+/-}$ = 6. [Student's t-test; ** p< 0.01; * p< 0.05; Statistical summary in Supplementary table 1]. Abbreviations: WT, wild-type; AP2$\gamma^{+/-}$, AP2γ heterozygous knockout mice.
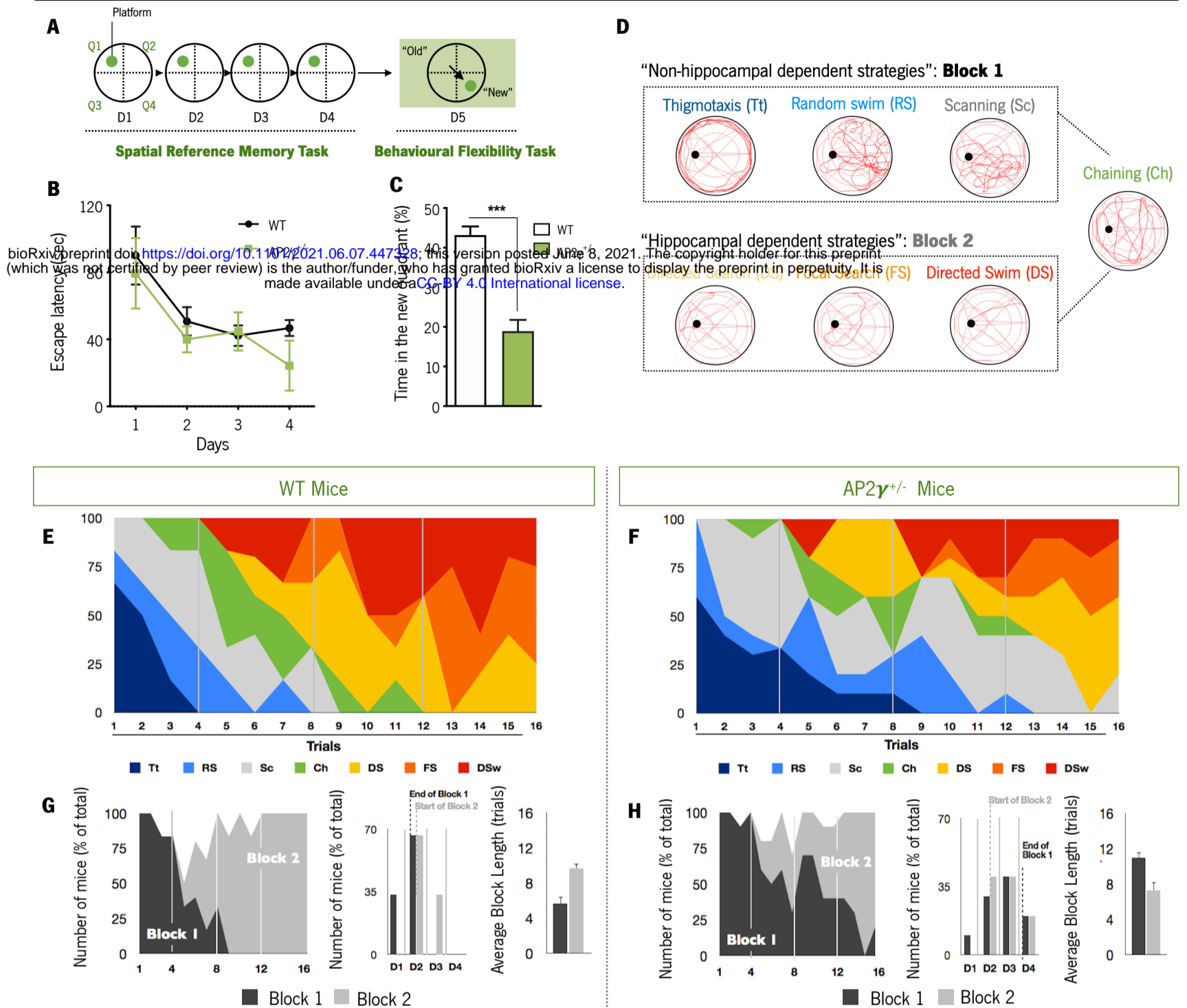
Water Maze Tasks

Figure 4: Cognitive performance of adult mice in the Morris water maze test. (A and B) Spatial reference memory was assessed as the average escape latency to find a hidden and fixed platform in each test day. (C) In the testing day, animals were subjected to a reversal-learning task to test behavioral flexibility. (D) Schematic representation of typical strategies to find the platform during spatial memory evaluation grouped according to its dependence of the hippocampus (Block 1: Non-hippocampal dependent strategies; Block 2: Hippocampal dependent strategies). Average of each strategy used for WT (E) and AP2$\gamma^{+/-}$ (F) mice, by trial number. The prevalence of each block along with trials, the distribution of strategies-block boundaries, and overall block length are shown for (G) WT and (F) AP2$^{+/-}$ mice. Data presented as mean SEM. n_{WT} = 10; $n_{AP2\gamma^{+/-}}$ = 10. [Repeated measures ANOVA and Student's t-test; ***p< 0.001; Statistical summary in Supplementary table 1]. Abbreviations: WT, wild-type; AP2$\gamma^{+/-}$, AP2γ heterozygous knockout mice.
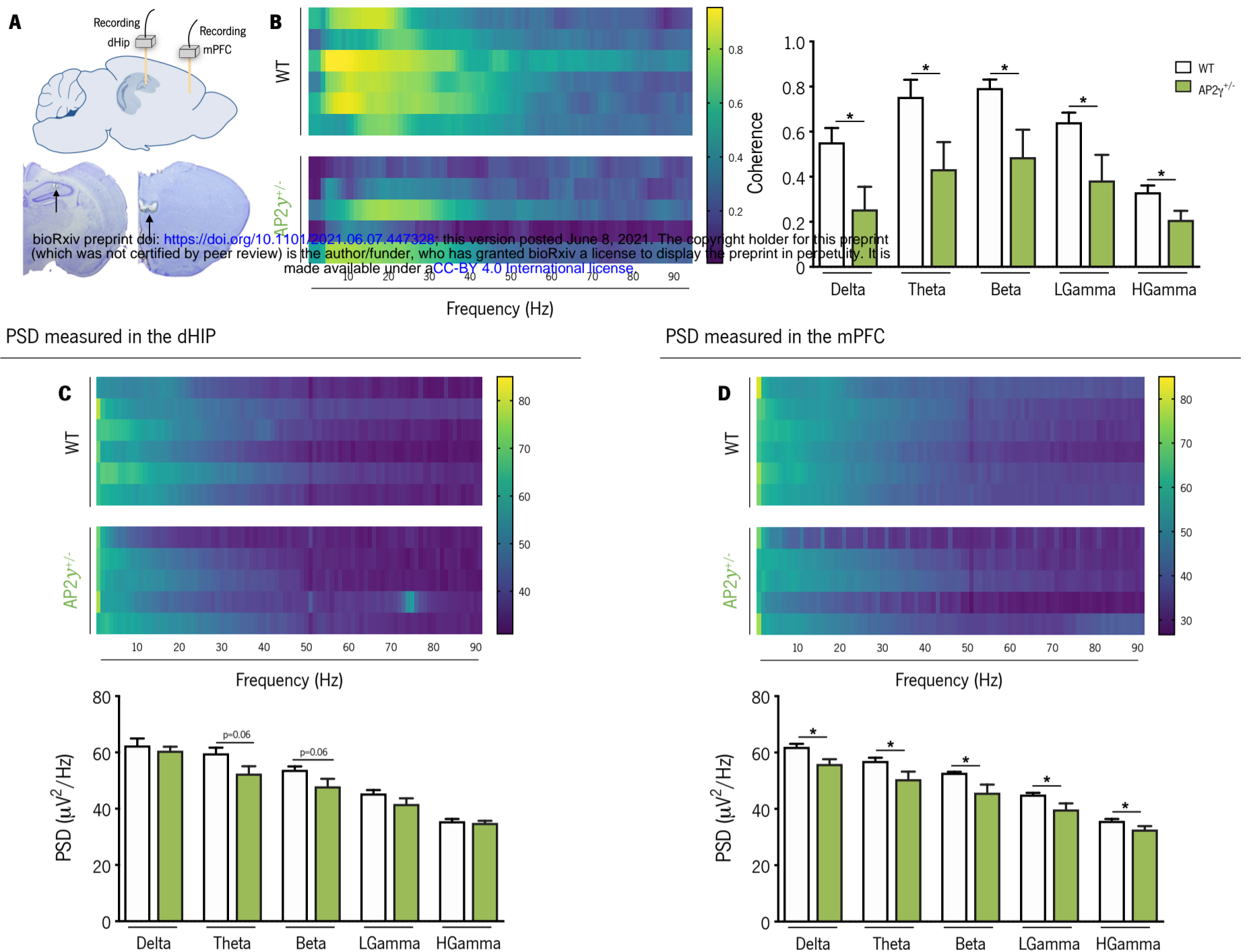
Figure 5: AP2γ deficiency induces deficits in spectral coherence between the dorsal hippocampus (dHip) and the medial prefrontal cortex (mPFC), impacting neuronal activity. (A) Identification of the local field potential (LFP) recording sites, with a depiction of the electrode positions (upper panel), and representative Cresyl violet-stained sections, with arrows indicating electrolytic lesions at the recording sites (lower panel). (B) Spectral coherence between the dHip and mPFC (left panel). Group comparison of the coherence values for each frequency (right panel). (C) Power spectral density (PSD) was measured in the dHip (C) and mPFC (D). Heatmaps of PSD activity (upper panel) and group comparison for each frequency (lower panel). Each horizontal line in the Y-axis of the presented spectrograms represents an individual mouse. Frequency bands range: delta (1-4Hz), theta (4-12 Hz), beta (12-20 Hz), low gamma (20-40 Hz), and High gamma (40-90 Hz). Data presented as mean SEM. n_{WT} = 6; $n_{AP2\gamma^{+/-}}$ = 5. [Student's t-test; *$p < 0.05$; Statistical summary in Supplementary table 1]. Abbreviations: WT, wild-type; AP2γ$^{+/-}$, AP2γ heterozygous knockout mice.
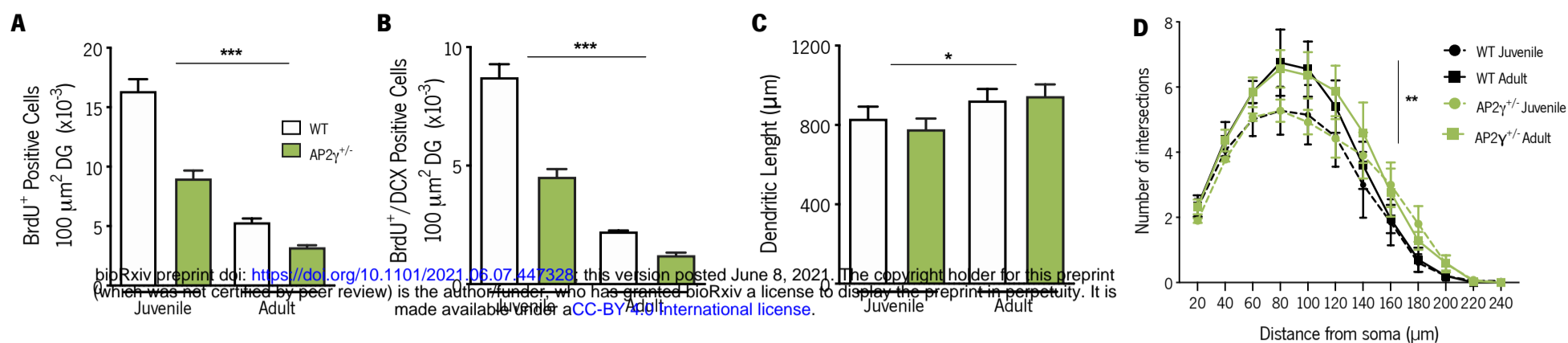
Supplementary Table 1: Statistical summary of results

Experiment	Figure(s)	Statistical details
Western blot protein quantifications	**Figure 1C**	**AP2γ quantification:** Student's t-test, $t_{6}=$ 2.90, $p<$ 0.01 **Sox2 quantification:** Student's t-test, $t_6=$ 1.02, $p=$ 0.35 **Pax6 quantification:** Student's t-test, $t_6=$ 2.60, $p<$ 0.01 **Tbr2 quantification:** Student's t-test, $t_6=$ 3.87, $p<$ 0.01 $n_{WT\ juvenile}$ = 4; $n_{AP2\gamma^{+/-}\ juvenile}$ = 4
	Figure 1D	**AP2γ quantification:** Student's t-test, $t_{6}=$ 5.19, $p<$ 0.001 **Sox2 quantification:** Student's t-test, $t_6=$ 1.02, $p=$ 0.35 **Pax6 quantification:** Student's t-test, $t_6=$ 6.62, $p<$ 0.01 **Tbr2 quantification:** Student's t-test, $t_6=$ 3.87, $p<$ 0.01 $n_{WT\ adult}$ = 4; $n_{AP2\gamma^{+/-}\ adult}$ = 4
Cell proliferation	**Figure 1F**	**BrdU⁺ cells:** Student's t-test, $t_{10}=$ 2.47, $p<$ 0.05 $n_{WT\ juvenile}$ = 6; $n_{AP2\gamma^{+/-}\ juvenile}$ = 6;
	Figure 1G	**BrdU⁺DCX⁺cells:** Student's t-test, $t_{10}=$ 2.58, $p<$ 0.05 $n_{WT\ juvenile}$ = 6; $n_{AP2\gamma^{+/-}\ juvenile}$ = 6;
	Figure 1H	**BrdU⁺ cells:** Student's t-test, $t_8=$ 2.67, $p<$ 0.05 $n_{WT\ adult}$ = 5; $n_{AP2\gamma^{+/-}\ adult}$ = 5
	Figure 1I	**BrdU⁺DCX⁺cells:** Student's t-test, ⁺: $t_8=$ 3.90, $p<$ 0.01 $n_{WT\ adult}$ = 5; $n_{AP2\gamma^{+/-}\ adult}$ = 5
	Supplementary Figure 1A	**BrdU⁺ cells:** Two-way ANOVA, $F_{(1,18)}=$ 147.8, $p<$0.001 Bonferroni's multiple comparisons test: Juvenile ₩ₜ vs Adult ₩ₜ: p<0.001 Juvenile $_{AP2\gamma^{+/-}}$ vs Adult $_{AP2\gamma^{+/-}}$: p<0.001 $n_{WT\ juvenile}$ = 6; $n_{WT\ juvenile}$ = 5 $n_{AP2\gamma^{+/-}\ juvenile}$ = 6; $n_{AP2\gamma^{+/-}\ adult}$ = 5
	Supplementary Figure 1B	**BrdU⁺DCX⁺cells:** Two-way ANOVA, $F_{(1,18)}=$ 186.5, $p<$0.001 Bonferroni's multiple comparisons test: Juvenile ₩ₜ vs Adult ₩ₜ: p<0.001 Juvenile $_{AP2\gamma^{+/-}}$ vs Adult $_{AP2\gamma^{+/-}}$: p<0.001 $n_{WT\ juvenile}$ = 6; $n_{WT\ juvenile}$ = 5 $n_{AP2\gamma^{+/-}\ juvenile}$ = 6; $n_{AP2\gamma^{+/-}\ adult}$ = 5

3D neuronal reconstruction	**Figure 1J**	**Dendritic length:** Student's t-test, t_6= 0.65, p= 0.52 $n_{WT\ juvenile}$ = 4; $n_{AP2\gamma^{+/-}\ juvenile}$ = 4
	Figure 1K	**Dendritic length:** Student's t-test, t_7= 0.27, p= 0.79 $n_{WT\ adult}$ = 4; $n_{AP2\gamma^{+/-}\ adult}$ = 5
	Supplementary Figure 1C	**Dendritic length:** Two-way ANOVA, $F_{(1,108)}$= 4.68, $p<$ 0.05 Bonferroni's multiple comparisons test: Juvenile $_{WT\ vs}$ Adult $_{WT}$: p<0.05 Juvenile $_{AP2\gamma^{+/-}\ vs}$ Adult $_{AP2\gamma^{+/-}}$: p<0.05 $n_{WT\ juvenile}$ = 4; $n_{AP2\gamma^{+/-}\ juvenile}$ = 4 $n_{WT\ adult}$ = 4; $n_{AP2\gamma^{+/-}\ adult}$ = 5
	Supplementary Figure 1D	**Neuronal arborization:** Genotype's comparison (WT vs AP2$\gamma^{+/-}$): Juvenile phase: Repeated measures ANOVA, $F_{(1,72)}$= 1.20, p= 0.28 Adulthood: Repeated measures ANOVA, $F_{(1,84)}$= 1.12, p= 0.29 Timepoints comparison (juvenile vs adulthood): Two-way ANOVA, $F_{(3,156)}$= 4.273, $p<$ 0.001 Bonferroni's multiple comparisons test: Juvenile $_{WT\ vs}$ Adult $_{WT}$: p<0.001 Juvenile $_{AP2\gamma^{+/-}\ vs}$ Adult $_{AP2\gamma^{+/-}}$: p<0.001 $n_{WT\ juvenile}$ = 4; $n_{WT\ adult\ juvenile}$ = 5 $n_{AP2\gamma^{+/-}\ juvenile}$= 4; $n_{AP2\gamma^{+/-}\ adult}$ = 5
OF (juvenile)	**Figure 2B and Supplementary Figure 3A**	**Distance in center:** Student's t-test, t_{20} = 2.15, p<0.05 **Average velocity:** Student's t-test, t_{22}= 0.16, p= 0.87 $n_{WT\ juvenile}$ = 13; $n_{AP2\gamma^{+/-}\ juvenile}$ = 11
TST (juvenile)	**Figure 2C**	**Immobility time:** Student's t-test, t_{27}= 0.23, p= 0.82 $n_{WT\ juvenile}$ = 15; $n_{AP2\gamma^{+/-}\ juvenile}$ = 10
SST (juvenile)	**Figure 2D**	**Grooming time:** Student's t-test, t_{23}= 0.05, p= 0.96 $n_{WT\ juvenile}$ = 4; $n_{AP2\gamma^{+/-}\ juvenile}$ = 4
ORT (juvenile)	**Figure 2F and G**	**Object location exploration:** Student's t-test, t_{15}= 0.24, p=0.81 **Object recognition exploration:** Student's t-test, t_{15}= 2.55, p<0.05 $n_{WT\ juvenile}$ = 11; $n_{AP2\gamma^{+/-}\ juvenile}$ = 8
OF	**Figure 3B; Supplementary Figure 4A**	**Distance in center:** Student's t-test, t_{18}= 2.10, p= 0.05

(adult)		**Average velocity:**
		Student's t-test, t_{24}=0.49, p= 0.63
		n_{WT} = 12; $n_{AP2\gamma}^{+/-}$ = 14
EPM (adult)	**Figure 3C**	**Open arms time:**
		Student's t-test, t_{18}= 3.10, p< 0.01
		n_{WT} = 12; $n_{AP2\gamma}^{+/-}$ = 14
FST (adult)	**Figure 3D**	**Immobility time:**
		Student's t-test, t_{24}= 0.61, p= 0.55
		n_{WT} = 12; $n_{AP2\gamma}^{+/-}$ = 14
TST (adult)	**Figure 3E**	**Immobility time:**
		Student's t-test, t_{10}= 0.64, p= 0.54
		n_{WT} = 6; $n_{AP2\gamma}^{+/-}$ $_{juvenile}$ = 6
ORT (adult)	**Figure 3F and G**	**Object location exploration:**
		Student's t-test, t_{23}= 1.80, p= 0.08
		Object recognition exploration:
		Student's t-test; t_{13}= 0.27, p= 0.79
		$n_{WT\ juvenile}$ = 12; $n_{AP2\gamma}^{+/-}$ $_{juvenile}$ = 9
CFC (adult)	**Figure 3I – K**	**Context probe A:**
		Student's t-test, t_{10}= 2.60, p< 0.05
		Context probe B:
		Student's t-test, t_{11}= 0.75, p= 0.75
		Cue Probe:
		Student's t-test, t_{11}= 1.26, p= 0.24
		$n_{WT\ juvenile}$ = 7; $n_{AP2\gamma}^{+/-}$ $_{juvenile}$ = 6
MWM (adult)	**Figure 4B and 4C; Supplementary figure 4C**	**Spatial Reference memory task:**
		Repeated measures ANOVA, $F_{(1,72)}$= 1.35, p= 0.25
		Behavior flexibility:
		Student's t-test, t_{18}= 6.79, p <0.001
		Working memory task:
		Repeated measures ANOVA, $F_{(1,72)}$= 0.85, p= 0.36
Spectral coherence dHip-mPFC	**Figure 5B**	**Delta:**
		Student's t-test, t_9= 2.61, p< 0.05
		Theta:
		Student's t-test, 2.34, p< 0.05
		Beta:
		Student's t-test, t_9= 2.62, p< 0.05
		Low gamma:
		Student's t-test, t_9= 2.30, p< 0.05
		High gamma:
		Student's t-test, t_9= 2.50, p< 0.05
		n_{WT} = 6; $n_{AP2\gamma}^{+/-}$ = 5
PSD values dHIP	**Figure 5C**	**Delta:**
		Student's t-test, t_9= 0.64, p= 0.54
		Theta:
		Student's t-test, t_9= 2.24, p= 0.06

		Beta:
		Student's t-test, t_9= 2.15, p= 0.06
		Low gamma:
		Student's t-test, : t_9= 1.66, p= 0.13
		High gamma:
		Student's t-test, t_9= 0.55, p= 0.60
		n_{WT} = 6; $n_{AP2\gamma}^{+/-}$ = 5
PSD values mPFC	**Figure 5D**	**Delta:**
		Student's t-test, t_9= 3.17, p< 0.05
		Theta:
		Student's t-test, t_9= 2.40, p< 0.05
		Beta:
		Student's t-test, t_9= 2.71, p< 0.05
		Low gamma:
		Student's t-test, : t_9= 2.55, p< 0.05
		High gamma:
		Student's t-test, t_9= 2.29, p< 0.05
		n_{WT} = 6; $n_{AP2\gamma}^{+/-}$ = 5
Spectral coherence vHIP-mPFC	**Supplementary figure 5B**	**Delta:**
		Student's t-test, t_9= 1.52, p= 0.17
		Theta:
		Student's t-test, t_9= 0.86, p= 0.42
		Beta:
		Student's t-test, t_9= 0.39, p= 0.70
		Low gamma:
		Student's t-test, t_9= 0.64, p= 0.54
		High gamma:
		Student's t-test, t_9= 0.95, p= 0.37
		n_{WT} = 5; $n_{AP2\gamma}^{+/-}$ = 5
PSD values vHIP	**Supplementary figure 5C**	**Delta:**
		Student's t-test, t_9= 1.74, p= 0.12
		Theta:
		Student's t-test, t_9= 1.22, p= 0.26
		Beta:
		Student's t-test, t_9= 0.12, p= 0.92
		Low gamma:
		Student's t-test, t_9= 0.19, p= 0.86
		High gamma:
		Student's t-test, t_9= 0.31, p= 0.23
		n_{WT} = 5; $n_{AP2\gamma}^{+/-}$ = 5

DG neuronal proliferation

DG neuronal morphology

DG neuronal complexity

**Supplementary figure 1: Comparative analysis of neural stem cells (NSC) proliferation and maturation in the hippocampal dentate gyrus (DG) at juvenile and adult periods.** Cell counts of BrdU positive (A) and BrdU/DCX double-positive (B) cells. Dendritic length (C) and complexity (D) of hippocampal granular neurons in juvenile and adult mice. Data presented as mean SEM. Sample size: Immunostainings assays: $n_{WT\ juvenile}$ = 6; $n_{AP2\gamma^{+/-}\ juvenile}$ = 6; $n_{WT\ adult}$ = 5; $n_{AP2\gamma^{+/-}\ adult}$ = 5; 3D neuronal reconstruction: $n_{WT\ juvenile}$ = 4; $n_{AP2\gamma^{+/-}\ juvenile}$ = 4; $n_{WT\ adult}$ = 4; $n_{AP2\gamma^{+/-}\ adult}$ = 5. [Two-way ANOVA and Repeated measures ANOVA, Statistical summary in Supplementary table 1] ***$p<0.001$, ** $p< 0.01$; * $p< 0.05$. Abbreviations: WT, wild-type; AP2$\gamma^{+/-}$, AP2γ heterozygous knockout mice.
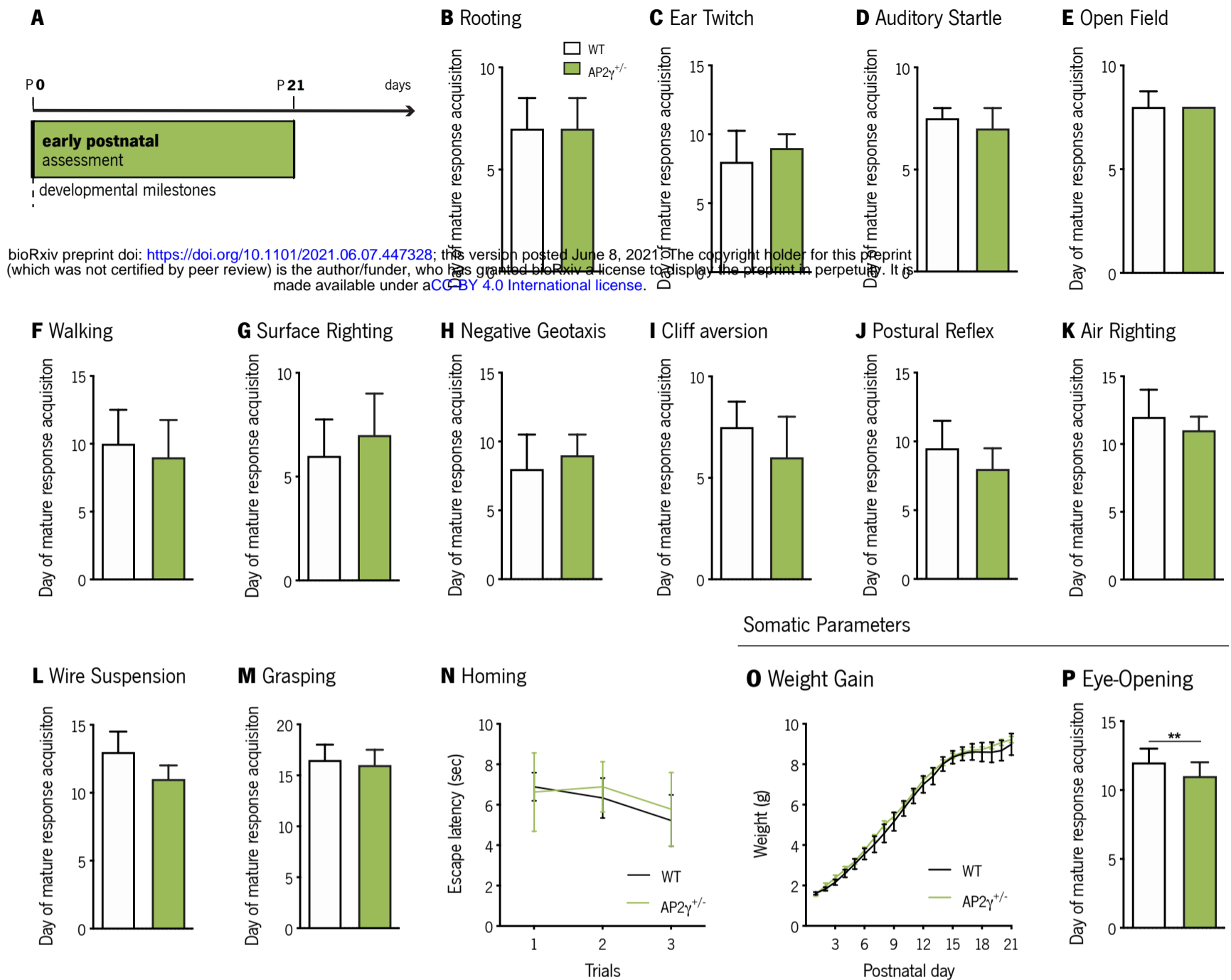
Supplementary figure 2: AP2γ constitutive and heterozygous deficiency does not impact on early postnatal development. (A) Timeline of early development assessment. (B-N) Set of established protocols to analyze the acquisition of mature responses, in neurobiological reflexes related to tactile (B and C) and auditory reflexes (D), motor function (E and F), vestibular system formation (G-K), strength (L and M), and olfactory maturation (N). Somatic parameters were also assessed. (O) Bodyweight gain from postnatal day (PND) 1 to PND 21 of WT and AP2γ$^{+/-}$ mice. (P) Eye-opening day. For the weight gain pattern, data presented as mean SEM; for the remaining tests, data was plotted as median IQR. Sample Size: n_{WT} = 9; $n_{AP2}$$^{+/-}$ = 9. [Mann-Whitney and Repeated measures ANOVA, ** p< 0.01, Statistical summary in Supplementary table 1]. Abbreviations: WT, wild-type; AP2γ$^{+/-}$, AP2γ heterozygous knockout mice; IQR, Interquartile range.

Open Field Test
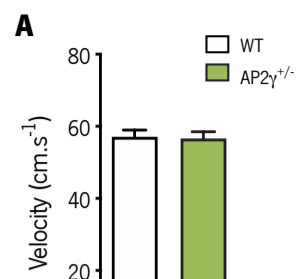
A

Supplementary figure 3: AP2γ deficiency does not impact on motor function in juvenile mice. (A) Average velocity assessed through the open field (OF) test in juvenile mice. Data presented as mean ± SEM. Sample Size: OF: n_{WT} = 13; $n_{AP2\gamma}{}^{+/-}$ = 11. [Student's t-test, Statistical summary in Supplementary table 1]. Abbreviations: WT, wild-type; AP2$\gamma^{+/-}$, AP2γ heterozygous knockout mice.

Open Field Test | Water Maze Task

A

**B**

C

Working Memory Task
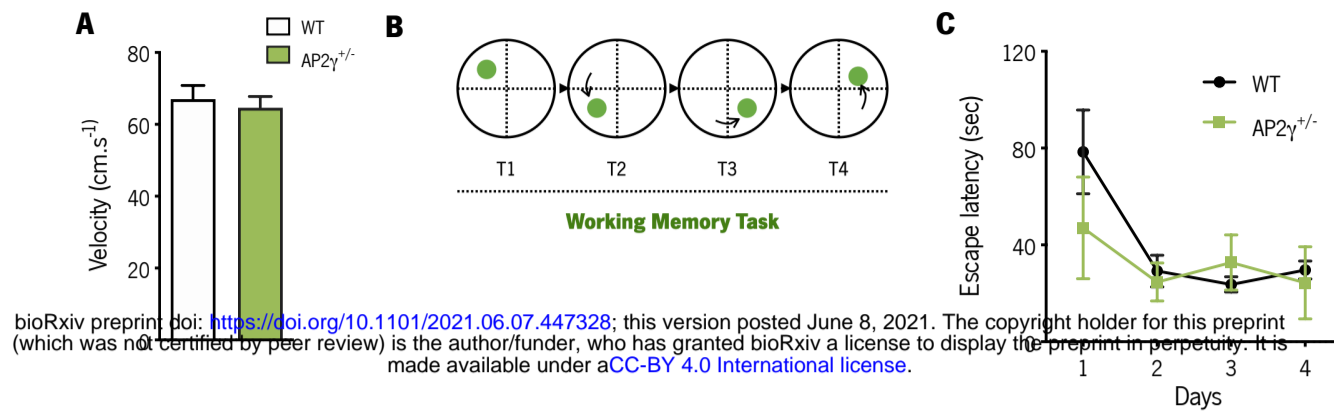
Supplementary figure 4: Deficiency in AP2γ transcription factor levels does not impact motor function, nor specific modalities of cognitive behavior. (A) Average velocity assessed through the open field (OF) test in adult mice. (B) Working memory task evaluated in the Morris water maze (MWM) test. Data presented as mean SEM. Sample size: OF: n_{WT} = 12; $n_{AP2\gamma}^{+/-}$ = 14; MWM: n_{WT} = 10; $n_{AP2\gamma}^{+/-}$ = 10. [Student's t-test and Repeated measures ANOVA, Statistical summary in Supplementary table 1]. Abbreviations: WT, wild-type; AP2$\gamma^{+/-}$, AP2γ heterozygous knockout mice.

Coherence between vHip and mPFC
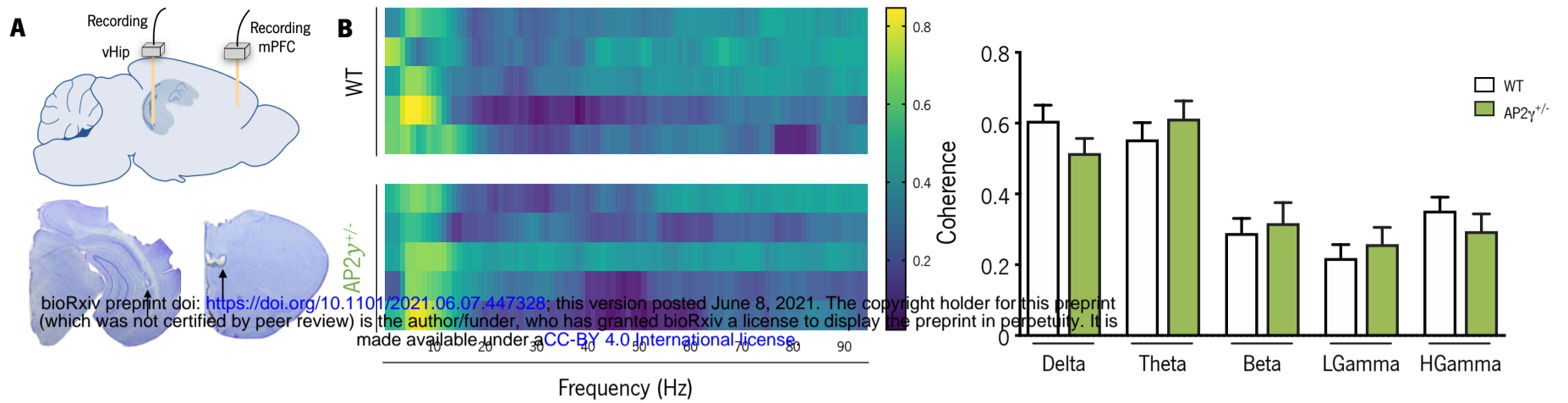
PSD measured in the vHIP
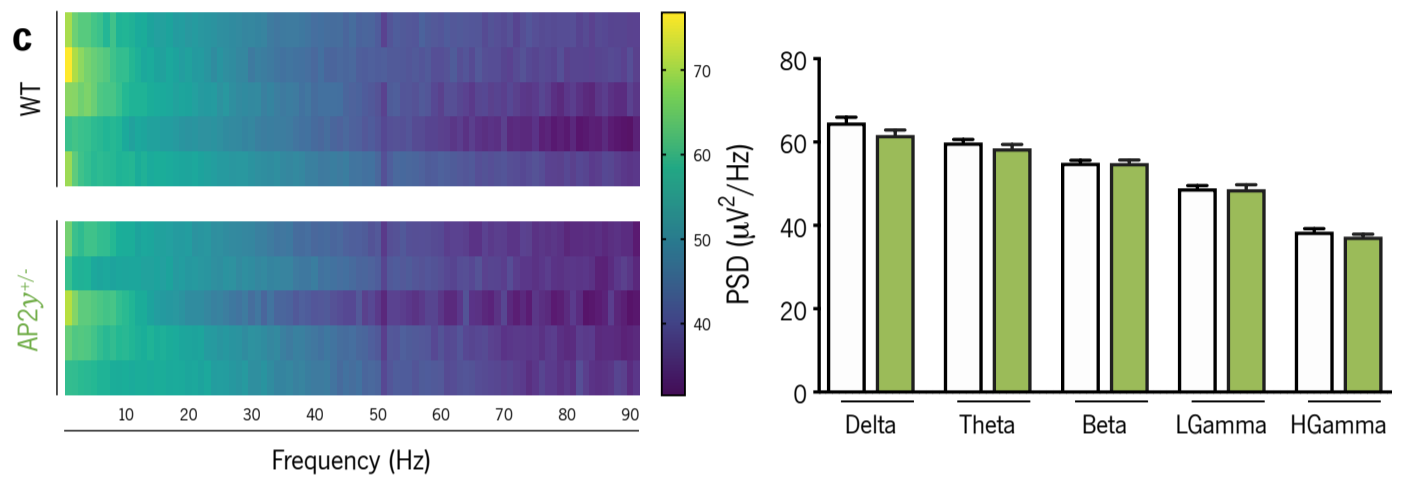
Supplementary figure 5: AP2γ deficiency does not impact neither on spectral coherence between the ventral hippocampus (vHip) and the medial prefrontal cortex (mPFC), nor the neuronal activity in each region. (A) Local field potentials (LFP) recording sites, with a depiction of the electrode positions (upper panel), and representative Cresyl violet-stained section (lower panel). (B) Spectral coherence (left panel) and group comparison for each frequency (right panel), between the vHip and mPFC of adult WT and AP2γ$^{+/-}$ mice. (C) Power spectral density (PSD) (upper panel), and group comparison of the PSD values in the vHip for each frequency (lower panel). In spectrograms, each horizontal line in the Y-axis represents an individual mouse. Frequency bands range: delta (1-4Hz), theta (4-12 Hz), beta (12-20 Hz), low gamma (20-40 Hz), and High gamma (40-90 Hz). Data presented as mean SEM. n_{WT} = 5; $n_{AP2γ^{+/-}}$ = 5. [Student's t-test, Statistical summary in Supplementary table 1]. Abbreviations: WT, wild-type; AP2γ$^{+/-}$, AP2γ heterozygous knockout mice; vHip, ventral hippocampus; mPFC, medial prefrontal cortex.